Semivisible dark photon in a model with vectorlike leptons for the $(g-2)_{e,\mu}$ and W-boson mass anomalies

Waleed Abdallah,[1,*] Mustafa Ashry,[1,†] Junichiro Kawamura,[2,‡] and Ahmad Moursy[3,§]

[1]Department of Mathematics, Faculty of Science, Cairo University, Giza 12613, Egypt
[2]Center for Theoretical Physics of the Universe, Institute for Basic Science (IBS), Daejeon 34051, Korea
[3]Department of Basic Sciences, Faculty of Computers and Artificial Intelligence, Cairo University, Giza 12613, Egypt

(Received 25 August 2023; accepted 9 January 2024; published 31 January 2024)

We propose a model that realizes a semivisible dark photon which can contribute to the anomalous magnetic moment $(g-2)$ of both electron and muon. In this model, the electron $g-2$ is deviated from the Standard Model (SM) prediction by the 1-loop diagrams involving the vectorlike leptons, while that of muon is deviated due to a nonvanishing gauge kinetic mixing with photons. We also argue that the W-boson mass can be deviated from the SM prediction due to the vectorlike lepton loops, so that the value obtained by the CDF II experiment can be explained. Thus, this model simultaneously explains the recent three anomalies in $g-2$ of electron and muon as well as the W-boson mass. The constraints on the $\mathcal{O}(1)$ GeV dark photon can be avoided because of the semivisible decay of the dark photon, $A' \to 2N \to 2\nu 2\chi \to 2\nu 4e$, where N is a SM singlet vectorlike neutrino and χ is a CP-even Higgs boson of the $U(1)'$ gauge symmetry.

DOI: 10.1103/PhysRevD.109.015031

I. INTRODUCTION

There is a long-standing discrepancy in the anomalous magnetic moment $(g-2)$ of muon between the Standard Model (SM) prediction [1–20] and the experimental measurement [21,22]. The latest world average of Δa_μ reports the 5.1σ discrepancy [23],

$$\Delta a_\mu := a_\mu^{\rm exp} - a_\mu^{\rm SM} = 2.49(48) \times 10^{-9}, \qquad (1.1)$$

whereas the recent lattice calculation [24] and the experiment determination [25] of the hadron vacuum polarization contribution to the muon $g-2$ point the value closer to the SM prediction, and hence the tension relaxes to a few sigma level. Nonetheless, we shall assume that the discrepancy is given by Eq. (1.1), since the current situation is not conclusive. The electron $g-2$ may also deviate from the SM prediction according to the recent precise measurement of the fine-structure constant using Cs atoms [26], and the discrepancy is given by [27]

$$\Delta a_e := a_e^{\rm exp} - a_e^{\rm SM} = -8.7(3.6) \times 10^{-13}, \qquad (1.2)$$

and hence there is a 2.4σ discrepancy from the experimental value [28,29]. Similarly to the muon $g-2$, however, the situation is not conclusive because the fine-structure constant determined by Rb atoms shows the value consistent with the SM [30]. Nonetheless, we also assume that there is the discrepancy in Eq. (1.2), especially the negative sign of its discrepancy. Simultaneous explanations for both anomalies have been studied in Refs. [26,27,31–44].

The model with a $U(1)'$ gauge symmetry and the vectorlike fourth family is studied in Refs. [45,46],[1] to explain the muon $g-2$ and another anomaly in the $b \to s\ell\ell$ process [59–68].[2] In these works, the $U(1)'$ gauge boson is assumed to be heavier than 100 GeV, so the gauge boson is called a Z' boson. The muon $g-2$ is explained by the 1-loop diagrams involving the vectorlike leptons via mixing with muons. In this case, however, the electron $g-2$ cannot be explained simultaneously because it causes the lepton flavor violations if the mixing with electrons is introduced. Reference [70] shows the W-boson mass measured by the CDF II [71],

$$m_W^{\rm CDF} = 80.4335(94)\ {\rm GeV}, \qquad (1.3)$$

*awaleed@sci.cu.edu.eg
†mustafa@sci.cu.edu.eg
‡junkmura13@gmail.com
§a.moursy@fci-cu.edu.eg

[1]Other types of models with vectorlike fermions and a $U(1)'$ are studied in Refs. [47–58].

[2]The recent measurement of $R_{K^{(*)}}$ shows the consistent value with the SM prediction [69].

which is larger than the previous measurements $m_W^{\rm PDG} = 80.379(12)$ GeV and the SM prediction $m_W^{\rm SM} = 80.361(6)$ GeV [72], can be explained by the 1-loop diagrams involving the vectorlike leptons lighter than about 200 GeV.

In this work, we study a new parameter space of the model proposed in Refs. [45,46], where the $U(1)'$ gauge boson is much lighter than the Z-boson mass and therefore we call it a dark-photon A' throughout this work. In such a scenario, the dark photon can explain Δa_μ if it is lighter than $\mathcal{O}(1)$ GeV and its gauge kinetic mixing with the photon is $\mathcal{O}(10^{-5}$–$10^{-2})$ depending on the dark-photon mass [73]. Note that the dark-photon contribution from the gauge kinetic mixing cannot explain the negative shift of the electron $g-2$ in Eq. (1.2), since it is predicted to be positive. In this model, we can explain Δa_e by the 1-loop diagrams involving the vectorlike leptons as for Δa_μ in the heavy Z' scenario [45,46], without lepton flavor violations. We also point out that the W-boson mass measured by the CDF II can be explained in the same manner as in Ref. [70]. Altogether, we study the light dark-photon region of the model in Refs. [45,46] in order to explain both electron and muon $g-2$, as well as m_W measured by the CDF II experiment without extending the model.

The dark photon explaining Δa_μ is excluded by the experiments if it decays dominantly to e^+e^- [74–76] or invisible particles [77,78]. This limit will be relaxed and the dark-photon explanation is still viable if the dark photon decays to both visible and invisible particles [79–83], namely if the dark photon is semivisible. Interestingly, in this model, the SM singlet vectorlike neutrino N can be lighter than the dark photon, and then N can decay to the $U(1)'$ breaking Higgs boson χ whose dominant decay mode is e^+e^-. Thus, the decay of the dark-photon A' proceeds as $A' \to 2N \to 2\nu\, 2\chi \to 2\nu\, 4e$, which is a semivisible decay.

The paper is organized as follows. In Sec. II, we briefly review the model with particular interests in the gauge kinetic mixing. We study the observables, including Δa_e, Δa_μ, and m_W in Sec. III, and then discuss signals from the dark photon in Sec. IV. Finally, we draw our conclusions in Sec. V. The details of the model and the loop functions for the oblique parameters are, respectively, in Appendixes A and B.

II. THE MODEL

We review the model proposed in Refs. [45,46] in which the SM is extended by a $U(1)'$ gauge symmetry and a family of vectorlike leptons. The matter contents of the model is summarized in Table I.

TABLE I. Quantum numbers of the scalars and leptons in the model under the gauge symmetry $SU(2)_L \times U(1)_Y \times U(1)'$. The index $i = 1, 2, 3$ runs over the three generations of the SM leptons.

Gauge symmetry	ℓ_{L_i}	$\bar{e}_{R_i}$	H	L_L	$\bar{E}_R$	$\bar{L}_R$	E_L	$\bar{N}_R$	N_L	Φ
$SU(2)_L$	**2**	**1**	**2**	**2**	**1**	**2**	**1**	**1**	**1**	**1**
$U(1)_Y$	−1	2	−1	−1	2	1	−2	0	0	0
$U(1)'$	0	0	0	−1	1	1	−1	1	−1	−1

A. Gauge boson sector

Unlike the studies in Refs. [45,46], we explicitly introduce the gauge kinetic mixing of the $U(1)'$ and $U(1)_Y$ symmetries. The gauge kinetic terms are given by

$$\mathcal{L}_{\rm gauge} = -\frac{1}{4}F_{\mu\nu}F^{\mu\nu} - \frac{1}{4}F'_{\mu\nu}F'^{\mu\nu} - \frac{\epsilon}{2}F'_{\mu\nu}F^{\mu\nu} - \frac{1}{4}G^a_{\mu\nu}G^{a\mu\nu}, \tag{2.1}$$

where $F_{\mu\nu}$, $F'_{\mu\nu}$, and $G^a_{\mu\nu}$ are the gauge-field strengths of $U(1)_Y$, $U(1)'$ and $SU(2)_L$, respectively. Here, ϵ is the gauge kinetic mixing factor. We denote the neutral vector fields of $U(1)_Y$, $U(1)'$, and $SU(2)_L$ by B_μ, V_μ, and W^3_μ, respectively. After the symmetry breaking by the SM Higgs boson and the $U(1)'$ breaking scalar Φ, the mass-squared matrix for (W^3_μ, B_μ, V_μ) is given by

$$\mathcal{M}^2_V = m_W^2 \begin{pmatrix} 1 & -t_W & 0 \\ -t_W & t_W^2 & 0 \\ 0 & 0 & t_V^2 \end{pmatrix}, \tag{2.2}$$

where $t_W := g_1/g_2$ and $t_V := m_V/m_W$ with $m_W := g_2 v_H/\sqrt{2}$ and $m_V = \sqrt{2} g' v_\Phi$. Here, g_1, g_2, and g' are, respectively, the gauge-coupling constants of $U(1)_Y$, $SU(2)_L$, and $U(1)'$. The canonically normalized mass basis of the gauge bosons are defined as

$$\begin{pmatrix} W^3_\mu \\ B_\mu \\ V_\mu \end{pmatrix} =: \begin{pmatrix} s_W & c_W C_{WA'} & c_W C_{WZ} \\ c_W & -s_W C_{BA'} & -s_W C_{BZ} \\ 0 & C_{VA'} & C_{VZ} \end{pmatrix} \begin{pmatrix} A_\mu \\ A'_\mu \\ Z_\mu \end{pmatrix}. \tag{2.3}$$

For $\epsilon, t_V \ll 1$, $C_{WA'}$, $C_{BA'}$, $C_{VZ} \sim \mathcal{O}(\epsilon)$ and C_{WZ}, C_{BZ}, $-C_{VA'} \sim 1 + \mathcal{O}(\epsilon^2)$. In this limit,

$$m^2_{A'} \sim m^2_V(1 + c^2_W \epsilon^2), \qquad m^2_Z \sim \frac{m^2_W}{c^2_W}(1 + s^2_W \epsilon^2), \tag{2.4}$$

where $s_W := g_1/\sqrt{g_1^2 + g_2^2} =: t_W c_W$. The explicit form of these matrices is shown in Appendix A.

B. Fermion sector

In the gauge basis, the relevant part of the Lagrangian specifying the mass terms of the vectorlike leptons and their Yukawa interactions are given by

$$\begin{aligned}\mathcal{L} \supset\ & m_L \bar{L}_R L_L + m_E \bar{E}_R E_L + m_N \bar{N}_R N_L \\ & + \bar{e}_{Ri} y^e_{ij} \ell_{Lj} H + \Phi \lambda^L_i \bar{L}_R \ell_{Li} - \Phi^* \lambda^E_i \bar{e}_{Ri} E_L \\ & + \lambda_e \bar{E}_R L_L H - \lambda'_e \bar{L}_R \tilde{H} E_L + \lambda_n \bar{N}_R L_L \tilde{H} \\ & + \lambda'_n \bar{L}_R H N_L + \text{H.c.} \end{aligned} \tag{2.5}$$

Here, $\tilde{H} = i\sigma_2 H^*$ and $i, j = 1, 2, 3$ label the SM generations. After the symmetry breaking via nonzero vacuum expectation values (VEVs) of the scalar fields, v_Φ and v_H, the mass matrices for $e_L = (e^-_{L_i}, L^-_L, E^-_L)$, $e_R = (e^-_{R_i}, E^-_R, L^-_R)$ and $n_L = (\nu_{L_i}, L^0_L, N_L)$, $n_R = (N_R, L^0_R)$ are given by

$$\mathcal{M}_e = \begin{pmatrix} y_{ij} v_H & 0 & \lambda_{L_i} v_\Phi \\ 0 & \lambda_e v_H & m_L \\ \lambda_{E_j} v_\Phi & m_E & \lambda'_e v_H \end{pmatrix},$$
$$\mathcal{M}_n = \begin{pmatrix} 0 & \lambda_{L_i} v_\Phi \\ \lambda_n v_H & m_L \\ m_N & \lambda'_n v_H \end{pmatrix}. \tag{2.6}$$

In this work, we do not explicitly introduce the right-handed neutrinos and treat neutrinos as massless particles. As shown in Ref. [46], the phenomenology will not be changed up to $\mathcal{O}(v_H/M_{\text{Maj}})$; when we introduce the heavy right-handed neutrinos with Majorana mass $M_{\text{Maj}} \sim 10^{10}$ GeV. The mass matrices are diagonalized as

$$U^\dagger_{e_L} \mathcal{M}_e U_{e_R} = \begin{pmatrix} m_{e_i} & 0 & 0 \\ 0 & m_{E_1} & 0 \\ 0 & 0 & m_{E_2} \end{pmatrix},$$
$$U^\dagger_{n_L} \mathcal{M}_n U_{n_R} = \begin{pmatrix} 0 & 0 \\ m_{N_1} & 0 \\ 0 & m_{N_2} \end{pmatrix}, \tag{2.7}$$

where $U_{e_{L,R}}$ and U_{n_L} (U_{n_R}) are 5×5 (2×2) unitary matrices. The leptons in the mass basis are defined as

$$\hat{e}_A = U^\dagger_{e_A} e_A, \qquad \hat{n}_A = U^\dagger_{n_A} n_A, \qquad A = L, R. \tag{2.8}$$

The Dirac fermions are defined as

$$[\psi_\ell]_J := \begin{pmatrix} [\hat{\ell}_L]_J \\ [\hat{\ell}_R]_J \end{pmatrix}, \quad \ell = e, n, \quad J = 1, 2, 3, 4, 5, \tag{2.9}$$

where $[\hat{n}_R]_j = 0$ for $j = 1, 2, 3$.

Throughout this work, we assume that the $U(1)'$ breaking scalar Φ exclusively couples to the first generation, i.e.,

$$\lambda_{L_i} =: \lambda_L \delta_{1i}, \qquad \lambda_{E_i} =: \lambda_E \delta_{1i}, \qquad \lambda_{N_i} =: \lambda_N \delta_{1i}, \tag{2.10}$$

so that the lepton flavor violations are not induced from the mixing. As we shall study the dark photon of $\mathcal{O}(1)$ GeV, the VEV of Φ is expected to be in this order, which is much smaller than that studied in Refs. [45,46]. In this regime, with omitting the mixing with the second and third generations, the diagonalization matrices are approximately given by

$$U_{e_L} = \begin{pmatrix} 1 & 0 & 0 \\ 0 & c_{e_L} & s_{e_L} \\ 0 & -s_{e_L} & c_{e_L} \end{pmatrix} \begin{pmatrix} 1 - (\eta^2_{L_1} + \eta^2_{L_2})/2 & \eta_{L_1} & -\eta_{L_2} \\ -\eta_{L_1} & 1 & 0 \\ \eta_{L_2} & 0 & 1 \end{pmatrix},$$
$$U_{e_R} = \begin{pmatrix} 1 & 0 & 0 \\ 0 & s_{e_R} & c_{e_L} \\ 0 & c_{e_R} & -s_{e_L} \end{pmatrix} \begin{pmatrix} 1 - (\eta^2_{R_1} + \eta^2_{R_2})/2 & -\eta_{R_1} & \eta_{R_2} \\ \eta_{R_1} & 1 & 0 \\ -\eta_{R_2} & 0 & 1 \end{pmatrix}, \tag{2.11}$$

where

$$\eta_{L_1} := c_{e_R} \lambda_L \frac{v_\Phi}{m_{E_1}}, \qquad \eta_{L_2} := s_{e_R} \lambda_L \frac{v_\Phi}{m_{E_2}},$$
$$\eta_{R_1} := s_{e_L} \lambda_E \frac{v_\Phi}{m_{E_1}}, \qquad \eta_{R_2} := c_{e_L} \lambda_E \frac{v_\Phi}{m_{E_2}}. \tag{2.12}$$

The first matrices diagonalize the right-lower 2×2 block of $\mathcal{M}_e$, and their analytical forms, as well as the diagonalization of the neutrino mass matrix, are shown in Appendix A. The second matrices approximately diagonalize the small off-diagonal elements of the electron and the vectorlike leptons up to the second order in $\eta := \mathcal{O}(\eta_{L_{1,2}}, \eta_{R_{1,2}})$.

C. Fermion interactions

The gauge interactions of the leptons with the neutral gauge bosons in the mass basis are given by

$$\begin{aligned}\mathcal{L}_{VF} =\ & \sum_{\ell=e,n} \bar{\psi}_\ell \gamma_\mu \sum_{A=L,R} \Bigg[e A^\mu Q_\ell \\ & + \sum_{X=A',Z} \frac{g_2}{c_W} X^\mu \Big\{ I_{\ell_A} (c^2_W C_{WX} + s^2_W C_{BX}) \\ & - s^2_W Q_\ell C_{BX} + \frac{c_W g'}{g_2} Q'_{\ell_A} C_{VX} \Big\} \Bigg] P_A \psi_\ell \\ =:\ & - e A^\mu \bar{\psi}_e \gamma^\mu \psi_e + \sum_{X=A',Z} \sum_{A=L,R} \sum_{\ell=e,n} X^\mu \bar{\psi}_\ell \gamma_\mu g^X_{\ell_A} P_A \psi_\ell, \end{aligned} \tag{2.13}$$

where

$$\begin{aligned} I_{e_A} &= -\frac{1}{2} U^\dagger_{e_A} \mathcal{P}_A U_{e_A} =: -\frac{1}{2} \mathcal{E}_A, \\ I_{n_A} &= +\frac{1}{2} U^\dagger_{n_A} \mathcal{P}_A U_{n_A} =: \frac{1}{2} \mathcal{N}_A, \\ Q'_{\ell_A} &= -U^\dagger_{\ell_A} \mathcal{P}' U_{\ell_A}, \end{aligned} \tag{2.14}$$

with $\mathcal{P}_R \coloneqq \mathrm{diag}(0,0,0,0,1) =: 1-\mathcal{P}_L$ and $\mathcal{P}' \coloneqq \mathrm{diag}(0,0,0,1,1)$. The electric coupling constant is defined as $e = g_1 g_2/\sqrt{g_1^2+g_2^2}$, and the electric charged are $Q_e = -1$ and $Q_n = 0$. The W-boson couplings are given by

$$\begin{aligned}\mathcal{L}_W &= \frac{g_2}{\sqrt{2}} W_\mu^- \bar{\psi}_n \gamma^\mu \sum_{A=L,R} h_A P_A \psi_e + \mathrm{H.c.} \\ &= \sum_{A=L,R} W_\mu^- \bar{\psi}_n \gamma^\mu g_A^W P_A \psi_e + \mathrm{H.c.}, \end{aligned} \tag{2.15}$$

where

$$h_A \coloneqq U_{n_A}^\dagger \mathcal{P}_A U_{e_A}. \tag{2.16}$$

The $U(1)'$ Higgs boson Φ is expanded as

$$\Phi = v_\Phi + \frac{1}{\sqrt{2}}(\chi + i a_\chi), \tag{2.17}$$

where a_χ is the Nambu-Goldstone boson absorbed by the dark-photon A'. The Yukawa interactions of the CP-even Higgs χ are given by

$$-\mathcal{L}_\chi = \frac{\chi}{\sqrt{2}} \sum_{\ell=e,n} \bar{\psi}_\ell Y_\ell^\chi P_L \psi_\ell + \mathrm{H.c.}, \tag{2.18}$$

where

$$\begin{aligned} Y_e^\chi &= U_{e_L}^\dagger \begin{pmatrix} 0 & 0 & \lambda_{L_i} \\ 0 & 0 & 0 \\ \lambda_{E_j} & 0 & 0 \end{pmatrix} U_{e_R}, \\ Y_n^\chi &= U_{n_L}^\dagger \begin{pmatrix} 0 & \lambda_{L_i} & \\ 0 & 0 & \\ 0 & 0 & \end{pmatrix} U_{n_R}. \end{aligned} \tag{2.19}$$

Up to $\mathcal{O}(\epsilon^2)$, the gauge couplings are given by

$$\begin{aligned} g_{\ell_A}^Z &\sim \frac{g_2}{c_W}(I_{\ell_A} - s_W^2 Q_\ell) + \epsilon s_W g' Q'_{\ell_A} \\ &\quad + \epsilon^2 g_2 t_W c_W \left\{ \frac{1}{2} I_{\ell_A} - Q_\ell \left(1 - \frac{s_W^2}{2}\right) \right\}, \end{aligned} \tag{2.20}$$

$$g_{\ell_A}^{A'} \sim -g' Q'_{\ell_A} \left(1 + \frac{c_W^2}{2}\epsilon^2\right) + \epsilon c_W s_W g_2 Q_\ell. \tag{2.21}$$

As explicitly shown in Appendix A, we find

$$\begin{aligned} \mathcal{E}_L &\sim \begin{pmatrix} 1-\eta_e^2/\lambda_E^2 & s_{e_L}\eta_e/\lambda_E & -c_{e_L}\eta_e/\lambda_E \\ s_{e_L}\eta_e/\lambda_E & c_{e_L}^2 & c_{e_L}s_{e_L} \\ -c_{e_L}\eta_e/\lambda_E & c_{e_L}s_{e_L} & s_{e_L}^2 \end{pmatrix}, \\ \mathcal{E}_R &\sim \begin{pmatrix} \eta_e^2/\lambda_L^2 & c_{e_R}\eta_e/\lambda_L & -s_{e_R}\eta_e/\lambda_L \\ c_{e_R}\eta_e/\lambda_L & c_{e_R}^2 & -c_{e_R}s_{e_R} \\ -s_{e_R}\eta_e/\lambda_L & -s_{e_R}c_{e_R} & s_{e_R}^2 \end{pmatrix}, \end{aligned} \tag{2.22}$$

where

$$\eta_e \coloneqq \lambda_L \lambda_E v_\Phi \left(\frac{s_{e_L} c_{e_R}}{m_{E_1}} + \frac{c_{e_L} s_{e_R}}{m_{E_2}} \right) \tag{2.23}$$

will appear in Δa_e expression in Sec. III. For the $U(1)'$ boson couplings,

$$\begin{aligned} Q'_{e_L} &\sim \begin{pmatrix} \eta_{L_1}^2 + \eta_{L_2}^2 & -\eta_{L_1} & \eta_{L_2} \\ -\eta_{L_1} & 1 & 0 \\ \eta_{L_2} & 0 & 1 \end{pmatrix}, \\ Q'_{e_R} &\sim \begin{pmatrix} \eta_{R_1}^2 + \eta_{R_2}^2 & \eta_{R_1} & -\eta_{R_2} \\ \eta_{R_1} & 1 & 0 \\ -\eta_{R_2} & 0 & 1 \end{pmatrix}. \end{aligned} \tag{2.24}$$

Hence, the Z-boson couplings to the SM leptons are shifted at $\mathcal{O}(\epsilon^2, \eta^2)$ and those of the dark-photon A' appears at ϵ with the subdominant contributions at $\mathcal{O}(\epsilon^2, \eta^2)$. The off-diagonal couplings of the SM leptons and the vectorlike ones are induced at $\mathcal{O}(\eta)$. The structures are similar for the couplings involving the neutral leptons. The Yukawa couplings of the χ boson is approximately given by

$$Y_e^\chi \sim \begin{pmatrix} 2\eta_e & c_{e_R}\lambda_L & -s_{e_R}\lambda_L \\ -s_{e_L}\lambda_E & \mathcal{O}(v_\Phi/m_{E_1}) & \mathcal{O}(v_\Phi/m_{E_1}) \\ c_{e_L}\lambda_E & \mathcal{O}(v_\Phi/m_{E_1}) & \mathcal{O}(v_\Phi/m_{E_2}) \end{pmatrix}. \tag{2.25}$$

III. ANOMALOUS MAGNETIC MOMENTS AND W-BOSON MASS

A. Anomalous magnetic moments

The 1-loop contribution to the anomalous magnetic moment of the lepton $\ell = e, \mu$ via the neutral gauge boson $X = Z, A'$ and the charged leptons is given by

$$\begin{aligned} \delta_X a_\ell = -\frac{m_\ell}{8\pi^2 m_X^2} \sum_{B=1}^{5} [&(|[g_{e_L}^X]_{i_\ell B}|^2 + |[g_{e_R}^X]_{i_\ell B}|^2) m_\ell F_Z(x_{e_B}^X) \\ &+ \mathrm{Re}([g_{e_L}^X]_{i_\ell B}[g_{e_R}^X]_{i_\ell B}^*) m_{e_B} G_Z(x_{e_B}^X)], \end{aligned} \tag{3.1}$$

where $x_{e_B}^X = m_{e_B}^2/m_X^2$. Here, m_{e_B} is the mass of the Bth-generation charged lepton, with flavor index $B = 1, \ldots, 5$. The index $i_\ell = 1, 2$ for $\ell = e, \mu$. The loop functions

$F_Z(x), G_Z(x)$ are defined in Appendix B. The 1-loop contribution from the χ scalar to Δa_ℓ is given by [84,85]

$$\delta_\chi a_\ell = -\frac{m_\ell}{32\pi^2 m_\chi^2}\sum_{B=1}^{5}[(|[Y_e^\chi]_{i_\ell B}|^2 + |[Y_e^\chi]_{Bi_\ell}|^2)m_\ell F_S(y_{e_B}^\chi) + \mathrm{Re}([Y_e^\chi]_{i_\ell B}[Y_e^\chi]_{Bi_\ell})m_{e_B}G_S(y_{e_B}^\chi)], \tag{3.2}$$

where $y_{e_B}^\chi := m_{e_B}^2/m_\chi^2$. Also, the loop functions $F_S(x)$, $G_S(x)$ are defined in Appendix B. Altogether, the new physics contribution to the anomalous magnetic moment is given by

$$\Delta a_\ell = \delta_{A'}a_\ell + \delta_Z a_\ell + \delta_\chi a_\ell - \delta_Z^{\mathrm{SM}} a_\ell, \tag{3.3}$$

where the SM contribution via the Z-boson loop,

$$\delta_Z^{\mathrm{SM}} a_\ell = -\frac{g_2^2 m_\ell^2}{8\pi^2 m_W^2}\left[\left(\frac{1}{4} - s_W^2 + 2s_W^4\right)F_Z(x_\ell^Z) + s_W^2\left(-\frac{1}{2} + s_W^2\right)G_Z(x_\ell^Z)\right], \tag{3.4}$$

is subtracted. The contributions from the Z, W, and Higgs bosons are negligible because the off-diagonal couplings in the mass basis are suppressed. The Feynman diagrams dominantly contribute to Δa_e and Δa_μ as shown in Fig. 1.

Let us estimate the sizes of Δa_ℓ in our model. From Eq. (2.20), the dark-photon contribution to Δa_μ is approximately given by

$$\Delta a_\mu \sim \delta_{A'}a_\mu \simeq -\frac{c_W^2 s_W^2 g_2^2 m_\mu^2 \epsilon^2}{8\pi^2 m_{A'}^2}(2F_Z(x_\mu^{A'}) + G_Z(x_\mu^{A'})) \tag{3.5}$$

$$\sim 2.8\times 10^{-9} \times \left(\frac{\epsilon}{0.02}\right)^2\left(\frac{1\,\mathrm{GeV}}{m_{A'}}\right)^2\left(\frac{2F_Z(x_\mu^{A'}) + G_Z(x_\mu^{A'})}{-2/3}\right). \tag{3.6}$$

Note that $2F_Z + G_Z$ is negative for $m_{A'} > m_\mu$.

It turns out that Δa_e is dominantly from the 1-loop diagrams involving the vectorlike leptons along with the dark photon or the χ boson, because of the chiral enhancement proportional to the vectorlike lepton masses. From Eqs. (2.20) and (2.24), we find

$$\Delta a_e \sim -\frac{m_e \eta_e}{16\pi^2 v_\Phi} \sim -3.2\times 10^{-13}\times\left(\frac{1\ \mathrm{GeV}}{v_\Phi}\right)\left(\frac{\eta_e}{10^{-7}}\right), \tag{3.7}$$

and η_e is approximately given by

$$\eta_e \sim \lambda_L\lambda_E\frac{\lambda_e v_H v_\Phi}{m_L m_E} \sim 1.7\times 10^{-7}\times\left(\frac{\lambda_e\lambda_L\lambda_E}{10^{-3}}\right)\left(\frac{v_\Phi}{1\,\mathrm{GeV}}\right)\left(\frac{10^3\,\mathrm{GeV}}{\sqrt{m_L m_E}}\right)^2, \tag{3.8}$$

for $v_H \ll m_E$. Thus, the vectorlike mass around the TeV scale can explain the deviation in Δa_e for the Yukawa coupling constants of $\mathcal{O}(0.1)$ and $v_\Phi \sim \mathcal{O}(1)\,\mathrm{GeV}$. Note that the contribution from the gauge kinetic mixing will be subdominant when Δa_μ is explained because the coupling induced by the kinetic mixing is flavor universal, and it is estimated as

$$\delta_{A'}a_e|_\epsilon = \frac{m_e^2}{m_\mu^2}\Delta a_\mu \simeq 5.8\times 10^{-14}\times\left(\frac{\Delta a_\mu}{2.51\times 10^{-9}}\right). \tag{3.9}$$

For $\eta_e \sim 10^{-7}$, the Z-boson couplings of the SM leptons are very close to the SM one since the deviation is at $\mathcal{O}(\eta_e^2)$; see Eq. (2.22).

Figure 2 shows the values of Δa_μ (left) and Δa_e (right) based on our numerical analysis. We see that Δa_μ is explained for $\epsilon \sim 0.02$ for the $1-\mathrm{GeV}$ dark photon as expected from Eq. (3.5). For $(\epsilon, m_{A'}) = (0.02, 1\ \mathrm{GeV})$, the vectorlike lepton masses are 1.5 TeV (500 GeV) with $\lambda_e = 0.1$ (0.01), as expected from Eqs. (3.7) and (3.8). Thus, our model provides a unified explanation for both Δa_e and Δa_μ without introducing lepton flavor violations.

B. W-boson mass

As shown in Refs. [70,86], the W-boson mass shift can be explained by the 1-loop effects of the fourth family vectorlike leptons. The T parameter [87,88] has a dominant contribution to this shift compared to the S, U parameters, and the T parameter is given by [89,90]

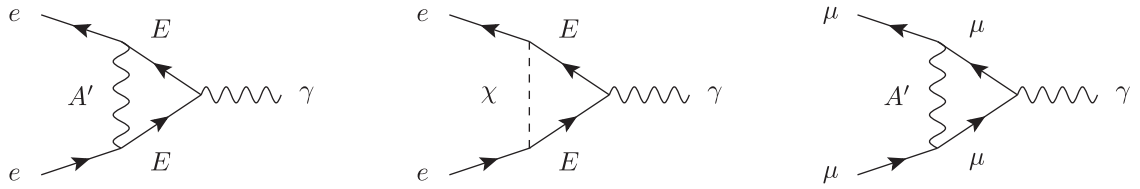

FIG. 1. The Feynman diagrams dominantly contribute to the Δa_e (left and middle) and Δa_μ (right).

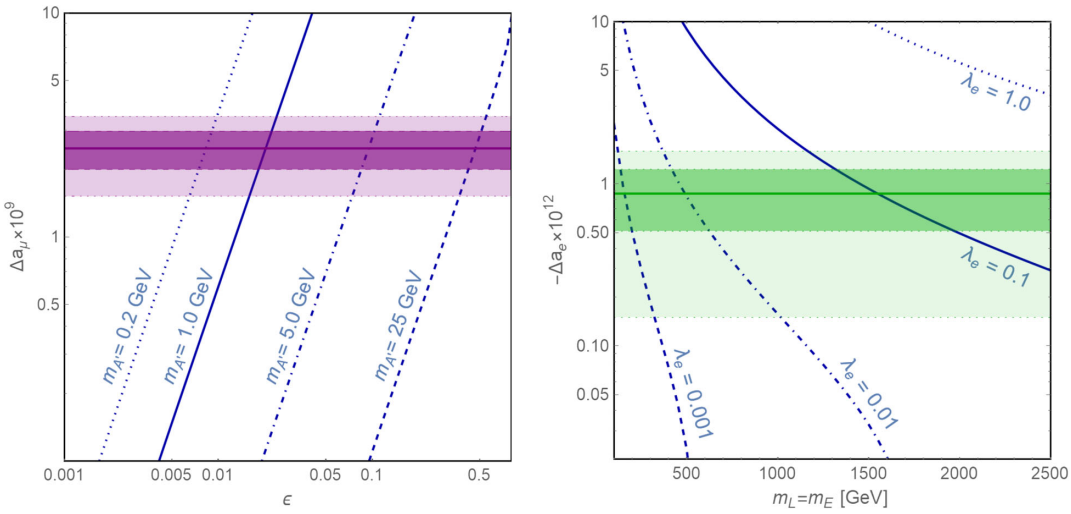

FIG. 2. The left panel shows ϵ versus Δa_μ with $m_{A'} = 0.2, 1, 5, 25$ GeV. The dark (light) purple region is the 1σ (2σ) range. The right panel shows $m_L = m_E$ versus $-\Delta a_e$ with $\lambda_e = 0.001, 0.01, 0.1, 1.0$. The dark (light) green region is the 1σ (2σ) range. The input parameters other than $m_L = m_E$ are chosen as the BP-A shown in Table II.

$$\begin{aligned}16\pi s_W^2 c_W^2 T = &\sum_{a,\beta}\{(|h^L_{a\beta}|^2 + |h^R_{a\beta}|^2)\theta_+(y_a, y_\beta) + 2\mathrm{Re}(h^L_{a\beta}h^{R*}_{a\beta})\theta_-(y_a, y_\beta)\}\\ &- \sum_{a<b}\{(|\mathcal{N}^L_{ab}|^2 + |\mathcal{N}^R_{ab}|^2)\theta_+(y_a, y_b) + 2\mathrm{Re}(\mathcal{N}^L_{ab}\mathcal{N}^{R*}_{ab})\theta_-(y_a, y_b)\}\\ &- \sum_{\alpha<\beta}\{(|\mathcal{E}^L_{\alpha\beta}|^2 + |\mathcal{E}^R_{\alpha\beta}|^2)\theta_+(y_\alpha, y_\beta) + 2\mathrm{Re}(\mathcal{E}^L_{\alpha\beta}\mathcal{E}^{R*}_{\alpha\beta})\theta_-(y_\alpha, y_\beta)\},\end{aligned} \tag{3.10}$$

where the indices a, b (α, β) run over the neutral (charged) leptons, and $y_a := m^2_{e_a}/m^2_Z$, $y_\alpha := m^2_{n_\alpha}/m^2_Z$. Here, $h^A_{a\beta} = [h_A]_{a\beta}$, $\mathcal{E}^A_{\alpha\beta} = [\mathcal{E}_A]_{\alpha\beta}$ and $\mathcal{N}^A_{ab} = [\mathcal{N}_A]_{ab}$ for $A = L, R$. The formula of $2\pi S$ can be obtained by replacing $\theta_\pm \to \psi_\pm$ ($\theta_\pm \to \chi_\pm$) in the first line (the second and third lines), while by replacing $\theta_\pm \to \chi_\pm$ the formula of $-2\pi U$ can be obtained. The loop functions are defined in Appendix B. The W-boson mass is given by [91,92]

$$\hat{m}^2_W = m^2_W|_{\mathrm{SM}}\left[1 + \frac{\alpha}{c^2_W - s^2_W}\left(-\frac{S}{2} + c^2_W T + \frac{c^2_W - s^2_W}{4s^2_W}U\right) + \Delta_W\right], \tag{3.11}$$

where

$$\Delta_W = \frac{c^2_W}{c^2_W - s^2_W}\left(-\frac{\Delta m^2_Z}{m^2_Z} + t^2_W \Delta h^L_{e\nu}\right) \tag{3.12}$$

is the tree-level contribution from the Z-boson mass-squared shift $\Delta m^2_Z/m^2_Z := m^2_Z/m^2_Z|_{\mathrm{SM}} - 1 \simeq s^2_W\epsilon^2$ due to the kinetic mixing and the W-boson coupling to the SM leptons $\Delta h^L_{e\nu} := 1 - [h_L]_{11} \sim \mathcal{O}(\eta^2)$.[3] The tree-level contributions are too small to explain the shift in the W-boson mass, and hence $T \sim \mathcal{O}(0.1)$ is necessary to explain the CDF II measurement. In fact, the limit on the dark-photon contributions to the Electroweak (EW) precision data is $\epsilon < 2.7 \times 10^{-2}$ for $m_{A'} \ll 10$ GeV [95], where the most important effect is from the shift of the Z-boson mass which results in the shift of the W-boson mass.

The T parameter is approximately given by

$$\begin{aligned}16\pi^2 c^2_W s^2_W T \simeq &\frac{4(\lambda'_n v_H)^4}{3m^2_L m^2_Z}\left[1 + \frac{1}{4}\left(\frac{\lambda'_e m_L}{\lambda'_n m_E}\right)^2\right.\\ &\left.\times\left\{2 - 6\log\frac{m^2_E}{m^2_L} + 3\left(\frac{\lambda'_e}{\lambda'_n}\right)^2\right\}\right],\end{aligned} \tag{3.13}$$

where we assume $m_N \ll v_H \ll m_L \ll m_E$ and $\lambda_e, \lambda_n \ll \lambda'_e, \lambda'_n$. The first term in the parentheses comes from the W-boson contributions involving N_2 and E_1, which are sensitive to

[3]The tree-level contributions can be absorbed into the oblique parameters [93,94], but our oblique parameters only include the loop effects from the vectorlike leptons, which are expected to be dominant.

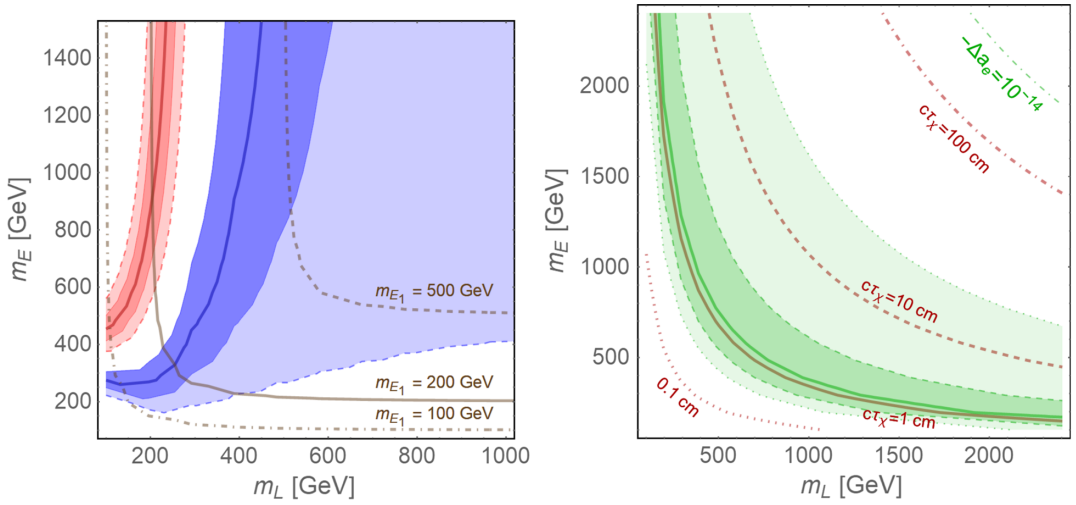

FIG. 3. Left: m_W is explained by the CDF II and PDG result within the 1σ (2σ) range in the darker (lighter) red and blue regions, respectively. The solid lines are the masses of the lightest charged exotic lepton $m_{E_1} = 100$, 200, and 500 GeV from bottom to top (left to right). The value of $\lambda_L = \lambda_E$ is chosen to explain Δa_e. Right: $\Delta a_e = -8.7 \times 10^{-13}$ on the green line, and it is within the 1σ (2σ) range in the darker (lighter) green region. The red lines are the length of flight of χ. Inputs are those at the benchmark point BP-B in Table II except (m_L, m_E) (and $\lambda_L = \lambda_E$) in the left (right) panel.

the mass difference in the doubletlike states. Since the second term is negative due to the logarithmic term, the T parameter slightly increases as it is suppressed by m_E. For $m_L \ll m_E$, the T parameter is estimated as

$$T \sim 0.1 \times \lambda_n'^4 \left(\frac{230\ \text{GeV}}{m_L}\right)^2. \tag{3.14}$$

Thus, the shift of the W-boson mass suggested by the CDF II measurement can be explained if $100 \lesssim m_L \lesssim 300$ GeV and $\lambda_n' \sim 1$, so that the mass split between the neutral and charged doubletlike states is sizable.[4]

In the left panel of Fig. 3, we plot the region where the W-boson mass is shifted due to the vectorlike lepton loops. The values favored by the CDF II and Particle Data Group (PDG) are explained in the 1σ (2σ) range in the darker (lighter) red and blue regions, respectively. In this plot, the input parameters except m_L, m_E, and $\lambda_L = \lambda_E$ are set to the values at the BP-B shown in Table II. The value of $\lambda_L = \lambda_E$ are chosen to explain $\Delta a_e \simeq -8.7 \times 10^{-13}$ based on the approximated formula in Eq. (3.7), and hence both Δa_e and Δa_μ are explained everywhere on the (m_L, m_E) plane. The CDF II value is explained if the doubletlike vectorlike lepton is about 200 GeV, while that of the PDG is explained at $m_L \sim 500$ GeV depending on the singlet mass m_E. We shall briefly discuss the LHC signals of the light vectorlike charged leptons in the next section.

[4]In models without the singlet vectorlike neutrino N, the split should be originated from the charged leptons, and thus the charged vectorlike lepton should be lighter than 200 GeV to explain the CDF II result [86].

Table II shows the three BPs, which explain both Δa_e and Δa_μ. At all points, $\epsilon = 0.02$ and $m_{A'} = 1$ GeV for $\Delta a_\mu \sim 2 \times 10^{-9}$. The Yukawa couplings and vectorlike masses are set to explain Δa_e. As discussed in the next section, we assume the spectrum $m_\chi < m_{N_1}/2 < m_{A'}$ to realize the semivisible dark photon compatible with the current limits. We also assume $\lambda_n \sim 0$ to keep m_{N_1} of $\mathcal{O}(1)$ GeV. At the BP-A, the vectorlike leptons are about 1.5 TeV, and hence the W-boson mass is very close to the SM value. At the BP-B (BP-C), the lightest charged lepton mass is about 300 (500) GeV, so that the W-boson mass favored by the CDF II (PDG) data is explained. We see that the W mass shift is dominantly explained by the T parameter, and the other oblique parameters, S and U, are much smaller.

IV. SIGNALS OF LIGHT PARTICLES

A. Semivisible dark photon

The experiments exclude the dark photon responsible for the muon anomalous magnetic moment if it decays to a pair of electrons or invisible particles [74–78]. The invisible dark photons are also searched in meson decays [96–99]. There are limits from deep inelastic scatterings independently to decays of the dark photon, and the current limit for $\mathcal{O}(1)$ GeV dark photon is $\epsilon \lesssim 0.035$ [100–104], which is larger than our benchmark points $\epsilon = 0.02$. However, the experiments lose sensitivity for the other semivisible dark-photon decay modes, as discussed in Refs. [79–82]. There is the experimental analysis searching for such dark photon at the fixed-target experiment NA64 [83]. According to Refs. [82,83], the dark-photon explanation for Δa_μ is viable for $m_{A'} \sim \mathcal{O}(0.1 - 1)$ GeV if the decay of heavy neutral

TABLE II. Values of the inputs and the outputs at the benchmark points. At all points, the other inputs not shown in the table are set to $\epsilon = 0.0203$, $\lambda_n = 0$, $(m_V, m_\chi, m_{N_1}) = (1.0, 0.3, 0.4)$ GeV, and $v_\Phi = 2\sqrt{2}$ GeV. The mass parameters are in the unit of GeV unless it is specified.

Inputs	A	B	C
(m_L, m_E)	(1500., 1500.)	(300., 1400.)	(500., 1400.)
$\lambda_L = \lambda_E$	0.2	0.25	0.3
λ_e	0.1	0.01	0.01
$\lambda'_e = \lambda'_n$	0.5	1.	1.
Outputs	**A**	**B**	**C**
(m_{E_1}, m_{E_2})	(1448., 1553.)	(297.4, 1411.)	(495.4, 1412.)
(m_{N_1}, m_{N_2})	(0.399, 1503.)	(0.346, 346.8)	(0.378, 529.4)
$-\Delta a_e \times 10^{13}$	9.326	7.698	6.557
$\Delta a_\mu \times 10^9$	2.488	2.488	2.488
m_W	80.3558	80.4046	80.3726
(S, T, U)	$(2.388, 2.039, -0.260)\times 10^{-4}$	(0.012, 0.111, 0.009)	(0.007, 0.041, 0.002)
$\Gamma_{A'}$ [MeV]	1.318	1.486	1.399
$\mathrm{Br}(A' \to N_1 N_1)$	0.9988	0.9989	0.9988
$c\tau_{N_1}$ [cm]	2.754	0.004444	0.006934
$\mathrm{Br}(N_1 \to \chi\nu)$	1.	1.	1.
$c\tau_\chi$ [cm]	1.078	1.541	2.065
$\mathrm{Br}(E_1 \to W N_1)$	0.7525	0.9216	0.9079
$\mathrm{Br}(E_1 \to A' e)$	0.1237	0.03918	0.04606
$\mathrm{Br}(E_1 \to \chi e)$	0.1237	0.03918	0.04606

fermion is fast enough. In our model, the dark photon will dominantly decay to a pair of vectorlike neutrinos N_1 if $2m_N < m_{A'}$. Then, the vectorlike neutrino N_1 will decay to the CP-even Higgs boson χ in the $U(1)'$ breaking scalar Φ. The scalar χ subsequently decays to a pair of electrons. Altogether, the decay chain of the dark photon is shown in Fig. 4:

$$A' \to N_1 N_1, \qquad N_1 \to \nu\chi, \qquad \chi \to ee, \tag{4.1}$$

which is kinematically allowed if $m_{A'}/2 > m_{N_1} > m_\chi > 2m_e$. There are two pairs of electrons in the final state accompanied with two neutrinos. Thus, the signal at the experiments will

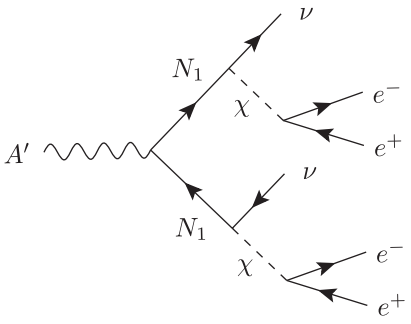

FIG. 4. Dominant dark-photon semivisible decay.

be semivisible if these decays happen inside detectors whose size is $\mathcal{O}(1m)$.

The first decay $A' \to N_1 N_1$ occurs promptly because $N_1 \sim N$ has the $U(1)'$ charge and there is the coupling without suppression from η. The second decay $N_1 \to \chi\nu$ is relatively long, but is short enough since the coupling is suppressed only by v_H/m_L. Note that the decay width of N_1 is too small if the scalar χ is much heavier than N_1 so that there are only three-body decays via A' or the SM bosons. The decay width of the scalar χ is approximately given by

$$\Gamma(\chi \to ee) = \frac{m_\chi}{16\pi} |[Y_e^\chi]_{ee}|^2 \left(1 - \frac{4m_e^2}{m_\chi^2}\right)^{3/2} \sim \frac{m_\chi}{4\pi}\eta_e^2. \tag{4.2}$$

Interestingly, this is directly related to the approximated formula of Δa_e in Eq. (3.7), so that the length of flight of χ is estimated as

$$c\tau_\chi \sim 1\ \mathrm{cm} \times \left(\frac{8.8\times 10^{-13}}{|\Delta a_e|}\right)^2 \left(\frac{0.4\ \mathrm{GeV}}{m_\chi}\right) \left(\frac{2\sqrt{2}\ \mathrm{GeV}}{v_\Phi}\right)^2. \tag{4.3}$$

Thus, the scalar χ decays before reaching or inside the detectors if $|\Delta a_e| \sim \mathcal{O}(10^{-13})$, whereas the decay cannot be detected and thus the signal is invisible if $|\Delta a_e| \ll 10^{-13}$.

The decay widths of A', N_1, and χ as well as the corresponding branching fractions at the BPs are shown in Table II. We see that the lifetime of A' and N_1 are (much) less than $\mathcal{O}(\mathrm{cm})$ and these dominantly decay to N_1N_1 and $\chi\nu$, respectively. Here, we calculated the two-body decays of A' to two leptons and that of N_1 to $\nu\chi$ on top of the three-body decays via the gauge bosons which are negligibly small because of the suppressed couplings and the kinetic suppression. Thus, we confirmed that the dark-photon decay can be dominated by $A' \to N_1N_1$, $N_1 \to \chi\nu$. If χ only decays to two electrons, the length of flight is $\mathcal{O}(1)$ cm, and hence this will be detected as prompt decay or displaced vertices depending on the detector design. It is also possible that the χ scalar decays to two pions if there are couplings in the quark sector as for the electrons. In this case, the lifetime would be shorter. In Ref. [82], the dark-photon decay proceeds as

$$A' \to \psi_i\psi_j, \psi_i \to \psi_{i-1}e^+e^-, \psi_j \to \psi_{j-1}e^+e^-, \ldots, \psi_2 \to \psi_1 e^+e^-, \tag{4.4}$$

where ψ_i's are neutral exotic fermion and ψ_1 is considered to be stable, so that it can be the dark matter. In this scenario, the neutral fermion ψ_i decays to three particles via off-shell dark photon, and thus their lifetimes tend to be longer than our case in which the decay chain $N_1 \to \nu\chi, \chi \to ee$ proceeds via only two-body decays. Furthermore, the energy deposits from the χ decay will be larger than those from the decays of ψ_i because of the larger phase space. Therefore, the signals from our dark photon will more easily evade the experimental limits searching for invisible dark photons. We expect that the dark photon of $\mathcal{O}(0.1-1)\,\mathrm{GeV}$ in our case will not be excluded by the current data. The simulation as done in Ref. [82] is beyond the scope of this work, but the simulation would confirm that the semivisible dark photon responsible for the lepton magnetic moments would not be excluded by the experiments.

B. The light vectorlike neutrino and $U(1)'$ scalar

In the realization of the semivisible dark photon, the vectorlike neutrino N_1 and the $U(1)'$ scalar χ should also be $\mathcal{O}(0.1\ \mathrm{GeV})$. The light vectorlike neutrino N_1 mixes with the SM neutrinos through the mixing induced by v_Φ and v_H. Using the results in Appendix A, the mixing between the light vectorlike neutrino and the electron neutrino is approximately given by

$$[h_L]_{eN_1} \sim \frac{\lambda_L\lambda_e'^2 v_\Phi v_H^2}{2m_L m_E^2} \sim 4\times10^{-6}\times\lambda_e'^2\left(\frac{\lambda_L}{0.3}\right)\left(\frac{v_\Phi}{1\ \mathrm{GeV}}\right)\left(\frac{500\ \mathrm{GeV}}{m_L}\right)\times\left(\frac{1500\ \mathrm{GeV}}{m_E}\right)^2, \tag{4.5}$$

where h_L is defined in Eq. (2.15), and thus this mixing is $\mathcal{O}(10^{-6})$ for our model. This is safely below the current experimental limits on the active-sterile mixing for $m_{N_1} \sim \mathcal{O}(0.1\ \mathrm{GeV})$; see Fig. 6 in Ref. [105].

In our model, the light scalar χ of mass $\sim\mathcal{O}(0.1\ \mathrm{GeV})$ is coupled to e^+e^- with a coupling strength estimated to be $2\eta_e \sim \mathcal{O}(10^{-7})$ from Eq. (3.8). Such a light scalar is constrained by the collider experimental limits searching for $e^+e^- \to \gamma\chi(\to e^+e^-)$ at *BABAR* [74,106], KLOE [107], Belle-II projection [108–110], and the electron beam-dump experiments [108,111]. Relevant to the light scalar mass range under consideration, these experiments impose an upper bound on its coupling with an e^+e^- pair, $Y_e^\chi \lesssim 10^{-3}$. The limit of $Y_e^\chi \lesssim 10^{-3}$ is obtained for $m_\chi \gtrsim 20$ MeV from *BABAR* [74] and Belle-II [108–110]. The beam-dump experiments [112–114] have sensitivities for $m_\chi \sim$ 1–200 MeV with $Y_e^\chi \sim 10^{-2} - 10^{-6}$, and no limits for heavier masses [111]. Therefore, our values are comfortably below this upper bound.

C. Vectorlike lepton search at the LHC

We briefly discuss the LHC limits for the charged vectorlike lepton E_1, which is expected to be light particularly to explain the W-boson mass shift. The vectorlike leptons might be excluded by the LHC limits. For the doubletlike leptons, the mass below 800 GeV is excluded if it decays to the SM particles [115,116]. In our model, however, the vectorlike lepton E_1 decays to WN_1, $A'e$, and/or χe, as discussed in Ref. [70]. The branching fractions of these decay modes of our BPs are shown in Table II. For the BPs, the dominant decay mode $E_1 \to WN_1$, followed by $N_1 \to \chi\nu \to ee\nu$, has at least two electrons in the final states. This case might be covered by the same search studied in Ref. [70], but there is no study for searching for the cascade decay. Thus, we cannot exclude this possibility. In addition, due to the many-body decay cascade, the phase space of the decay $E_1 \to WN_1$ is small and thus the many leptons in the final state are relatively soft. The subdominant decay modes $E_1 \to \chi e \to eee$ and $E_1 \to A'e \to eee$ have three electrons in the final state. These signals are similar to those from $E_1 \to Z'\mu \to \mu\mu\mu$, studied in Ref. [70], which excludes the vectorlike lepton masses up to 500 GeV for $\mathrm{Br}(E_1 \to eee) \sim 10\%$. For our BP-A, $\mathrm{Br}(E_1 \to eee) \simeq 12\%$ and $m_{E_1} \simeq 1.5$ TeV, which is safely above this limit. On the other hand, the limits for branching fractions less than 10% are not visible; therefore, the BP-B and BP-C whose $\mathrm{Br}(E_1 \to eee) \simeq 5\%$, may be allowed. We also note that this will not be the case if χ dominantly decays to quarks.[5]

[5]If χ couples with quarks, the precision measurements of kaon decays will constrain the χ as discussed in Ref. [117], depending on the flavor structure of the quark couplings. Also, the relation of the lifetime to Δa_e in Eq. (4.3) is changed by the mixing with quarks. A concrete study is beyond the scope of this paper.

V. CONCLUSIONS

In this work, we proposed a scenario in which both anomalies in electron and muon anomalous magnetic moments are explained without extending the model proposed in Refs. [45,46]. The discrepancy for electron, Δa_e, is explained by the 1-loop diagrams involving the dark photon and the vectorlike leptons, whereas that for muon, Δa_μ, is explained by the 1-loop diagrams induced by the gauge kinetic mixing with photons. Since the latter effect is always positive, we cannot consider the opposite case in which $\Delta a_e < 0$ is explained by the gauge kinetic mixing. Since two discrepancies are explained by the different origins, there are no lepton flavor violations induced by the new particles in the model. We also showed that the W-boson mass measured at the CDF II can be explained if the vectorlike lepton is below 300 GeV. Such a light vectorlike lepton would be excluded by the high-multiplicity lepton channels at the LHC, depending on its decay modes, as discussed in Sec. IV C. If the light vectorlike lepton is not excluded by the LHC, this model can address the three anomalies simultaneously.

The dark-photon explanation of Δa_μ is severely constrained by the experiments in the simplest setups. In our model, however, the dark photon can decay to a pair of vectorlike neutrinos, $A' \to N_1 N_1$, followed by the decays $N_1 \to \chi(\to ee)\nu$, so that the dark photon becomes semivisible which is not excluded by the dark-photon searches. We also find that the lifetime of the χ field is directly related to the new physics contribution to Δa_e, and thus our resolution to avoid the invisible dark-photons search works only if $|\Delta a_e| \gtrsim 10^{-14}$. This scenario would be probed by the direct searches for the semivisible dark photons, or pair productions of the charged vectorlike leptons at the LHC, which are subjects of our future works. Our model provides an explicit example of the semivisible dark photon relying only on two-body decays, which are qualitatively different from those considered in the literature.

ACKNOWLEDGMENTS

The work of J. K. is supported in part by the Institute for Basic Science (Grant No. IBS-R018-D1).

APPENDIX A: DETAILS OF THE MODEL

1. Diagonalization of vector boson mass matrix

We show the explicit form of the diagonalization matrix to obtain the canonically normalized mass basis of the vector bosons. We decompose the diagonalization matrix as

$$\begin{pmatrix} W_\mu^3 \\ B_\mu \\ V_\mu \end{pmatrix} =: \mathcal{E} R_1 R_2 \begin{pmatrix} A_\mu \\ A'_\mu \\ Z_\mu \end{pmatrix}, \tag{A1}$$

where $\mathcal{E}$ canonically normalizes the kinetic terms, R_1 block diagonalizes the massless photon and the others, and R_2 diagonalizes the 2×2 block of the massive bosons. Their explicit forms are given by

$$\begin{aligned} \mathcal{E} &= \frac{1}{\sqrt{2}} \begin{pmatrix} \sqrt{2} & 0 & 0 \\ 0 & \eta_+ & -\eta_- \\ 0 & \eta_+ & \eta_- \end{pmatrix}, \\ R_1 &= \frac{1}{\sqrt{2}} \begin{pmatrix} \sqrt{2}s_W & \sqrt{2}c_W & 0 \\ c_W/\eta_+ & -s_W/\eta_+ & 1/\eta_- \\ -c_W/\eta_- & s_W/\eta_- & 1/\eta_+ \end{pmatrix}, \\ R_2 &= \begin{pmatrix} 1 & 0 & 0 \\ 0 & c_V & s_V \\ 0 & -s_V & c_V \end{pmatrix}, \end{aligned} \tag{A2}$$

where $\eta_\pm := 1/\sqrt{1 \pm \epsilon}$ and

$$\begin{aligned} c_V &:= \sqrt{\frac{1}{2}\left(1 - \frac{1 - (1+s_W^2)\epsilon^2 - c_W^2 t_V^2}{\sqrt{d_V}}\right)}, \\ s_V &:= \mathrm{sign}(\epsilon)\sqrt{\frac{1}{2}\left(1 + \frac{1 - (1+s_W^2)\epsilon^2 - c_W^2 t_V^2}{\sqrt{d_V}}\right)}, \end{aligned} \tag{A3}$$

with

$$d_V := (1-\epsilon^2 c_W^2)^2 - 2\{1-(1+s_W^2)\epsilon^2\}c_W^2 t_V^2 + c_W^4 t_V^4. \tag{A4}$$

Altogether, the diagonalization matrix has the form

$$\begin{aligned} \mathcal{E} R_1 R_2 &= \begin{pmatrix} s_W & c_W c_V & c_W s_V \\ c_W & -s_W c_V + \epsilon s_V \eta_+ \eta_- & -s_V s_W - \epsilon c_V \eta_+ \eta_- \\ 0 & -s_V \eta_+ \eta_- & c_V \eta_+ \eta_- \end{pmatrix} \\ &=: \begin{pmatrix} s_W & c_W C_{WA'} & c_W C_{WZ} \\ c_W & -s_W C_{BA'} & -s_W C_{BZ} \\ 0 & C_{VA'} & C_{VZ} \end{pmatrix}. \end{aligned} \tag{A5}$$

The masses after diagonalization are given by

$$m_{A'}^2 = \frac{m_W^2}{2c_W^2(1-\epsilon^2)}(1 + c_W^2(t_V^2 - \epsilon^2) - \sqrt{d_V}), \tag{A6}$$

$$m_Z^2 = \frac{m_W^2}{2c_W^2(1-\epsilon^2)}(1 + c_W^2(t_V^2 - \epsilon^2) + \sqrt{d_V}). \tag{A7}$$

Up to the second order in ϵ and t_V,

$$\begin{aligned} &C_{WA'} \sim s_W \epsilon, \quad C_{BA'} \sim -\frac{c_W^2}{s_W}\epsilon, \quad C_{VA'} \sim -\left(1 + \frac{c_W^2}{2}\epsilon^2\right) \\ &C_{WZ} \sim 1 - \frac{s_W^2}{2}\epsilon^2, \quad C_{BZ} \sim 1 + \left(1 - \frac{s_W^2}{2}\right)\epsilon^2, \quad C_{VZ} \sim s_W \epsilon, \end{aligned} \tag{A8}$$

and

$$m_{A'}^2 \sim m_V^2(1+c_W^2\epsilon^2), \qquad m_Z^2 \sim \frac{m_W^2}{c_W^2}(1+s_W^2\epsilon^2). \tag{A9}$$

2. Diagonalization of the fermion mass matrices

We show the diagonalization matrices of the leptons,

$$\mathcal{M}_e = \begin{pmatrix} y_1 v_H & 0 & \lambda_L v_\Phi \\ 0 & \lambda_e v_H & m_L \\ \lambda_E v_\Phi & m_E & \lambda_e' v_H \end{pmatrix},$$
$$\mathcal{M}_n = \begin{pmatrix} 0 & \lambda_L v_\Phi \\ \lambda_n v_H & m_L \\ m_N & \lambda_n' v_H \end{pmatrix}, \tag{A10}$$

for $v_\Phi, m_N \ll v_H \lesssim m_L, m_E$. Here, we omit the second and third generations under the assumption of Eq. (2.10). We also assume that $m_L, m_E, m_N > 0$. The diagonalization matrices of the charged leptons are given by

$$U_{e_L} = \begin{pmatrix} 1 & 0 & 0 \\ 0 & c_{e_L} & s_{e_L} \\ 0 & -s_{e_L} & c_{e_L} \end{pmatrix} \begin{pmatrix} 1-(\eta_{L_1}^2+\eta_{L_2}^2)/2 & \eta_{L_1} & -\eta_{L_2} \\ -\eta_{L_1} & 1 & 0 \\ \eta_{L_2} & 0 & 1 \end{pmatrix},$$
$$U_{e_R} = \begin{pmatrix} 1 & 0 & 0 \\ 0 & s_{e_R} & c_{e_L} \\ 0 & c_{e_R} & -s_{e_L} \end{pmatrix} \begin{pmatrix} 1-(\eta_{R_1}^2+\eta_{R_2}^2)/2 & -\eta_{R_1} & \eta_{R_2} \\ \eta_{R_1} & 1 & 0 \\ -\eta_{R_2} & 0 & 1 \end{pmatrix}, \tag{A11}$$

up to the second order in $\eta \coloneqq \mathcal{O}(\eta_{L_{1,2}}, \eta_{R_{1,2}})$. The first matrices diagonalize the right-lower 2×2 block of $\mathcal{M}_e$. The angles are given by

$$c_{e_L} = \sqrt{\frac{1}{2}\left(1-\frac{T_{e_L}}{\sqrt{D_e}}\right)}, \qquad s_{e_L} = \sigma_{e_L}\sqrt{\frac{1}{2}\left(1+\frac{T_{e_L}}{\sqrt{D_e}}\right)},$$
$$c_{e_R} = \sqrt{\frac{1}{2}\left(1+\frac{T_{e_R}}{\sqrt{D_e}}\right)}, \qquad s_{e_R} = -\sigma_{e_R}\sqrt{\frac{1}{2}\left(1-\frac{T_{e_R}}{\sqrt{D_e}}\right)}, \tag{A12}$$

where

$$S_e \coloneqq m_E^2 + m_L^2 + (\lambda_e^2+\lambda_e'^2)v_H^2,$$
$$D_e \coloneqq S_e^2 - 4(m_L m_E - \lambda_e\lambda_e' v_H^2)^2,$$
$$T_{e_L} \coloneqq m_L^2 - m_E^2 + (\lambda_e^2-\lambda_e'^2)v_H^2,$$
$$T_{e_R} \coloneqq m_E^2 - m_L^2 + (\lambda_e^2-\lambda_e'^2)v_H^2, \tag{A13}$$

and

$$\sigma_{e_L} \coloneqq \mathrm{sign}(\lambda_e m_E + \lambda_e' m_L),$$
$$\sigma_{e_R} \coloneqq \mathrm{sign}(\lambda_e m_L + \lambda_e' m_E). \tag{A14}$$

The second matrices diagonalize the mixing between the first generation and the vectorlike lepton. The singular values are given by[6]

$$m_{e_1} \simeq y_1 v_H + v_\Phi \eta_e, \qquad m_{E_1} \simeq \sqrt{\frac{S_e - \sqrt{D_e}}{2}},$$
$$m_{E_2} \simeq \sqrt{\frac{S_e + \sqrt{D_e}}{2}}, \tag{A17}$$

where

$$\eta_e \coloneqq \lambda_L\lambda_E v_\Phi\left(\frac{s_{e_L}c_{e_R}}{m_{E_1}} + \frac{c_{e_L}s_{e_R}}{m_{E_2}}\right)$$
$$\sim \lambda_e\lambda_L\lambda_E\frac{v_\Phi v_H}{m_L m_E} + \mathcal{O}\left(\frac{v_H^3}{m_E^3}\right). \tag{A18}$$

For the neutrinos, the diagonalization matrices are given by

$$U_{n_L} = \begin{pmatrix} 1 & 0 & 0 \\ 0 & c_{L_1} & s_{L_1} \\ 0 & -s_{L_1} & c_{L_1} \end{pmatrix} \begin{pmatrix} c_{L_2} & s_{L_2} & 0 \\ -s_{L_2} & c_{L_2} & 0 \\ 0 & 0 & 1 \end{pmatrix} \begin{pmatrix} 1 & 0 & 0 \\ 0 & c_{n_L} & s_{n_L} \\ 0 & -s_{n_L} & c_{n_L} \end{pmatrix},$$
$$U_{n_R} = \begin{pmatrix} s_{n_R} & c_{n_R} \\ c_{n_R} & -s_{n_R} \end{pmatrix}, \tag{A19}$$

where

[6]The diagonal elements after the rotation by the first matrix are given by

$$\mu_{E_1} = \frac{\lambda_e v_H}{2c_{e_L}s_{e_R}}\left[1-\frac{1}{\sqrt{D_e}}\left\{S_e + 2\frac{\lambda_e'}{\lambda_e}(m_L m_E - \lambda_e\lambda_e' v_H^2)\right\}\right],$$
$$\mu_{E_2} = \frac{\lambda_e v_H}{2s_{e_L}c_{e_R}}\left[1+\frac{1}{\sqrt{D_e}}\left\{S_e + 2\frac{\lambda_e'}{\lambda_e}(m_L m_E - \lambda_e\lambda_e' v_H^2)\right\}\right], \tag{A15}$$

such that

$$\begin{pmatrix} c_{e_L} & s_{e_L} \\ -s_{e_L} & c_{e_L} \end{pmatrix}\begin{pmatrix} \lambda_e v_H & m_L \\ m_E & \lambda_e' v_H \end{pmatrix}\begin{pmatrix} s_{e_R} & c_{e_R} \\ c_{e_R} & -s_{e_R} \end{pmatrix} = \mathrm{diag}(\mu_{E_1}, \mu_{E_2}), \tag{A16}$$

where $\mu_{E_{1,2}}$ are, in general, not positive. Under the assumption, $m_L, m_E > 0$ and $v_H \ll m_E$, $\mu_{E_a} > 0$, and thus $\mu_{E_a} = m_{E_a}$ given by Eq. (A17).

$$c_{L_1} \coloneqq \frac{m_N}{\sqrt{m_N^2+\lambda_n^2 v_H^2}}, \qquad s_{L_1} \coloneqq \frac{\lambda_n v_H}{\sqrt{m_N^2+\lambda_n^2 v_H^2}},$$
$$c_{L_2} \coloneqq \frac{c_{L_1} m_L - s_{L_1}\lambda_n' v_H}{\tilde{m}_L}, \qquad s_{L_2} \coloneqq \frac{\lambda_L v_\Phi}{\tilde{m}_L}, \tag{A20}$$

with $\tilde{m}_L \coloneqq \sqrt{\lambda_L^2 v_\Phi^2 + (c_{L_1} m_L - s_{L_1}\lambda_n' v_H)^2}$. The first matrix is to rotate away the (2,1) element, and then the (1,2) element is rotated away by the second matrix. The angles in the last matrix, $c_{n_{L,R}}$ and $s_{n_{L,R}}$, are given by formally replacing $\lambda_e \to 0$, $m_E \to \sqrt{m_N^2+\lambda_n^2 v_H^2}$, $m_L \to \tilde{m}_L$ and $\lambda_e' v_H \to s_{L_1} m_L + c_{L_1}\lambda_n' v_H$ from $c_{e_{L,R}}$ and $s_{e_{L,R}}$ shown in Eq. (A12). The singular values m_{N_1} and m_{N_2} are, respectively, obtained by the same replacement from m_{E_1} and m_{E_2} in Eq. (A17). Note that the diagonalization for $\mathcal{M}_n$ is exact, not relying on any approximation.

For $v_H \ll m_E$ and $m_L < m_E$, the mixing angles are approximately given by

$$s_{e_L} \sim v_H \frac{\lambda_e m_E + \lambda_e' m_L}{|m_E^2 - m_L^2|}, \qquad s_{e_R} \sim -v_H \frac{\lambda_e m_L + \lambda_e' m_E}{|m_E^2 - m_L^2|}. \tag{A21}$$

The masses of the vectorlike leptons are given by

$$m_{E_1} \sim m_L - v_H^2 \frac{(\lambda_e^2+\lambda_e'^2) m_L + 2\lambda_e\lambda_e' m_E}{2(m_E^2 - m_L^2)},$$
$$m_{E_2} \sim m_E + v_H^2 \frac{(\lambda_e^2+\lambda_e'^2) m_E + \lambda_e\lambda_e' m_L}{2(m_E^2 - m_L^2)}, \tag{A22}$$

for $m_L < m_E$ and $m_E - m_L \gg v_H$. For the neutrinos, $\lambda_n v_H \lesssim m_N \lesssim \mathcal{O}(1)$ GeV is necessary to make the vectorlike neutrino N_1 light so that the dark photon can decay. We shall assume $\lambda_n = 0$ for simplicity. The neutrino mixing angles are approximately given by

$$c_{n_L} \sim \frac{\lambda_n' v_H}{\sqrt{m_L^2+\lambda_n'^2 v_H^2}}, \qquad s_{n_L} \sim \frac{m_L}{\sqrt{m_L^2+\lambda_n'^2 v_H^2}},$$
$$c_{n_R} \sim 0, \qquad s_{n_R} \sim -1, \tag{A23}$$

and the vectorlike neutrino masses are given by

$$m_{N_1} \simeq \frac{m_N m_L}{m_L^2+\lambda_n'^2 v_H^2}, \qquad m_{N_2} \simeq \sqrt{m_L^2+\lambda_n'^2 v_H^2}. \tag{A24}$$

3. Lepton couplings

The approximate forms of $\mathcal{E}_A$, $\mathcal{N}_A$, and h_A are given by

$$\mathcal{E}_L \sim \begin{pmatrix} 1-\eta_e^2/\lambda_E^2 & s_{e_L}\eta_e/\lambda_E & -c_{e_L}\eta_e/\lambda_E \\ s_{e_L}\eta_e/\lambda_E & c_{e_L}^2 & c_{e_L}s_{e_L} \\ -c_{e_L}\eta_e/\lambda_E & c_{e_L}s_{e_L} & s_{e_L}^2 \end{pmatrix}, \qquad \mathcal{E}_R \sim \begin{pmatrix} \eta_e^2/\lambda_L^2 & c_{e_R}\eta_e/\lambda_L & -s_{e_R}\eta_e/\lambda_L \\ c_{e_R}\eta_e/\lambda_L & c_{e_R}^2 & -c_{e_R}s_{e_R} \\ -s_{e_R}\eta_e/\lambda_L & -s_{e_R}c_{e_R} & s_{e_R}^2 \end{pmatrix},$$
$$\mathcal{N}_L \sim \begin{pmatrix} 1 & 0 & 0 \\ 0 & c_{n_L}^2 & c_{n_L}s_{n_L} \\ 0 & c_{n_L}s_{n_L} & s_{n_L}^2 \end{pmatrix}, \qquad \mathcal{N}_R = \begin{pmatrix} c_{n_R}^2 & -c_{n_R}s_{n_R} \\ -c_{n_R}s_{n_R} & s_{n_R}^2 \end{pmatrix}, \tag{A25}$$

$$h_L \sim \begin{pmatrix} 1-\frac{1}{2}(\eta_{L_1}^2+\eta_{L_2}^2+s_{L_2}^2)+s_{L_2}(c_{e_L}\eta_{L_1}-s_{e_L}\eta_{L_2}) & \eta_{L_1}-c_{e_L}s_{L_2} & -\eta_{L_2}-s_{e_L}s_{L_2} \\ c_{n_L}(s_{L_2}-c_{e_L}\eta_{L_1}+s_{e_L}\eta_{L_2}) & c_{e_L}c_{n_L} & s_{e_L}c_{n_L} \\ s_{n_L}(s_{L_2}-c_{e_L}\eta_{L_1}+s_{e_L}\eta_{L_2}) & c_{e_L}s_{n_L} & s_{e_L}s_{n_L} \end{pmatrix},$$
$$h_R \sim \begin{pmatrix} c_{n_R}(c_{e_R}\eta_{R_1}+s_{e_R}\eta_{R_2}) & c_{e_R}c_{n_R} & -c_{n_R}s_{e_R} \\ -s_{n_R}(c_{e_R}\eta_{R_1}+s_{e_R}\eta_{R_2}) & -c_{e_R}s_{n_R} & s_{e_R}s_{n_R} \end{pmatrix}, \tag{A26}$$

up to $\mathcal{O}(\eta^2)$ and $\mathcal{O}(s_{L_2}^2)$. Here, we take $s_{L_1} = 0$ and the subdominant contributions in the lower-right 2×2 block are omitted. For the Z'-boson couplings,

$$Q'_{e_L} \sim \begin{pmatrix} \eta_{L_1}^2+\eta_{L_2}^2 & -\eta_{L_1} & \eta_{L_2} \\ -\eta_{L_1} & 1 & 0 \\ \eta_{L_2} & 0 & 1 \end{pmatrix}, \qquad Q'_{e_R} \sim \begin{pmatrix} \eta_{R_1}^2+\eta_{R_2}^2 & \eta_{R_1} & -\eta_{R_2} \\ \eta_{R_1} & 1 & 0 \\ -\eta_{R_2} & 0 & 1 \end{pmatrix},$$
$$Q'_{n_L} \sim \begin{pmatrix} s_{L_2}^2 & -c_{n_L}s_{L_2} & -s_{n_L}s_{L_2} \\ -c_{n_L}s_{L_2} & 1 & 0 \\ -s_{n_L}s_{L_2} & 0 & 1 \end{pmatrix}, \qquad Q'_{n_R} = \begin{pmatrix} 1 & 0 \\ 0 & 1 \end{pmatrix}. \tag{A27}$$

The Yukawa couplings are given by

$$Y_e^\chi \sim \begin{pmatrix} 2\eta_e & c_{e_R}\lambda_L & -s_{e_R}\lambda_L \\ -s_{e_L}\lambda_E & \lambda_E s_{e_L}\eta_{R_1}+\lambda_L c_{e_R}\eta_{L_1} & -\lambda_E s_{e_L}\eta_{R_2}-\lambda_L s_{e_R}\eta_{L_1} \\ c_{e_L}\lambda_E & -\lambda_E c_{e_L}\eta_{R_1}-\lambda_L c_{e_R}\eta_{L_2} & \lambda_E c_{e_L}\eta_{R_2}+\lambda_L s_{e_R}\eta_{L_2} \end{pmatrix},$$
$$Y_n^\chi \sim \lambda_L \begin{pmatrix} c_{n_R} & -s_{n_R} \\ c_{n_L}c_{n_R}s_{L_2} & -c_{n_L}s_{n_R}s_{L_2} \\ s_{n_L}c_{n_R}s_{L_2} & -s_{n_L}s_{n_R}s_{L_2} \end{pmatrix}. \tag{A28}$$

APPENDIX B: LOOP FUNCTIONS

The loop functions for Δa_ℓ are given by

$$F_Z(x) = \frac{5x^4-14x^3+39x^2-38x+8-18x^2\ln(x)}{12(1-x)^4}, \qquad G_Z(x) = \frac{x^3+3x-4-6x\ln(x)}{2(1-x)^3}, \tag{B1}$$

and

$$F_S(y) = -\frac{y^3-6y^2+3y+6y\ln(y)+2}{6(1-y)^4}, \qquad G_S(y) = \frac{y^2-4y+2\ln(y)+3}{(1-y)^3}. \tag{B2}$$

The loop functions for the oblique parameters are given by

$$\theta_+(y_1,y_2) = y_1+y_2-\frac{2y_1y_2}{y_1-y_2}\log\frac{y_1}{y_2}, \qquad \theta_-(y_1,y_2) = 2\sqrt{y_1y_2}\left(\frac{y_1+y_2}{y_1-y_2}\log\frac{y_1}{y_2}-2\right), \tag{B3}$$

$$\chi_+(y_1,y_2) = \frac{y_1+y_2}{2}-\frac{(y_1-y_2)^2}{3}+\left(\frac{(y_1-y_2)^3}{6}-\frac{1}{2}\frac{y_1^2+y_2^2}{y_1-y_2}\right)\log\frac{y_1}{y_2}$$
$$+\frac{y_1-1}{6}f(y_1,y_1)+\frac{y_2-1}{6}f(y_2,y_2)+\left(\frac{1}{3}-\frac{y_1+y_2}{6}-\frac{(y_1-y_2)^2}{6}\right)f(y_1,y_2), \tag{B4}$$

$$\chi_-(y_1,y_2) = -\sqrt{y_1y_2}\left[2+\left(y_1-y_2-\frac{y_1+y_2}{y_1-y_2}\right)\log\frac{y_1}{y_2}+\frac{f(y_1,y_1)+f(y_2,y_2)}{2}-f(y_1,y_2)\right], \tag{B5}$$

and

$$\psi_+(y_1,y_2) = \frac{2y_1+10y_2}{3}+\frac{1}{3}\log\frac{y_1}{y_2}+\frac{y_1-1}{6}f(y_1,y_1)+\frac{5y_2+1}{6}f(y_2,y_2), \tag{B6}$$

$$\psi_-(y_1,y_2) = -\sqrt{y_1y_2}\left(4+\frac{f(y_1,y_1)+f(y_2,y_2)}{2}\right). \tag{B7}$$

Here, the function f is defined as

$$f(y_1,y_2)=\begin{cases}\sqrt{d}\log\left|\frac{y_1+y_2-1+\sqrt{d}}{y_1+y_2-1-\sqrt{d}}\right| & d>0\\ 0 & d=0\\ -2\sqrt{|d|}\left[\tan^{-1}\frac{y_1-y_2+1}{\sqrt{|d|}}-\tan^{-1}\frac{y_1-y_2-1}{\sqrt{|d|}}\right] & d<0\end{cases} \tag{B8}$$

with $d=(1+y_1-y_2)^2-4y_1$.

[1] T. Aoyama *et al.*, The anomalous magnetic moment of the muon in the Standard Model, Phys. Rep. **887**, 1 (2020).

[2] T. Aoyama, M. Hayakawa, T. Kinoshita, and M. Nio, Complete tenth-order QED contribution to the muon $g-2$, Phys. Rev. Lett. **109**, 111808 (2012).

[3] T. Aoyama, T. Kinoshita, and M. Nio, Theory of the anomalous magnetic moment of the electron, Atoms **7**, 28 (2019).

[4] A. Czarnecki, W. J. Marciano, and A. Vainshtein, Refinements in electroweak contributions to the muon anomalous magnetic moment, Phys. Rev. D **67**, 073006 (2003); Phys. Rev. D **73**, 119901(E) (2006).

[5] C. Gnendiger, D. Stöckinger, and H. Stöckinger-Kim, The electroweak contributions to $(g-2)_\mu$ after the Higgs boson mass measurement, Phys. Rev. D **88**, 053005 (2013).

[6] M. Davier, A. Hoecker, B. Malaescu, and Z. Zhang, Reevaluation of the hadronic vacuum polarisation contributions to the standard model predictions of the muon $g-2$ and $\alpha(m_Z^2)$ using newest hadronic cross-section data, Eur. Phys. J. C **77**, 827 (2017).

[7] A. Keshavarzi, D. Nomura, and T. Teubner, Muon $g-2$ and $\alpha(M_Z^2)$: A new data-based analysis, Phys. Rev. D **97**, 114025 (2018).

[8] G. Colangelo, M. Hoferichter, and P. Stoffer, Two-pion contribution to hadronic vacuum polarization, J. High Energy Phys. 02 (2019) 006.

[9] M. Hoferichter, B.-L. Hoid, and B. Kubis, Three-pion contribution to hadronic vacuum polarization, J. High Energy Phys. 08 (2019) 137.

[10] M. Davier, A. Hoecker, B. Malaescu, and Z. Zhang, A new evaluation of the hadronic vacuum polarisation contributions to the muon anomalous magnetic moment and to $\boldsymbol{\alpha(m_Z^2)}$, Eur. Phys. J. C **80**, 241 (2020).

[11] A. Keshavarzi, D. Nomura, and T. Teubner, $g-2$ of charged leptons, $\alpha(M_Z^2)$, and the hyperfine splitting of muonium, Phys. Rev. D **101**, 014029 (2020).

[12] A. Kurz, T. Liu, P. Marquard, and M. Steinhauser, Hadronic contribution to the muon anomalous magnetic moment to next-to-next-to-leading order, Phys. Lett. B **734**, 144 (2014).

[13] K. Melnikov and A. Vainshtein, Hadronic light-by-light scattering contribution to the muon anomalous magnetic moment revisited, Phys. Rev. D **70**, 113006 (2004).

[14] P. Masjuan and P. Sánchez-Puertas, Pseudoscalar-pole contribution to the $(g_\mu-2)$: A rational approach, Phys. Rev. D **95**, 054026 (2017).

[15] G. Colangelo, M. Hoferichter, M. Procura, and P. Stoffer, Dispersion relation for hadronic light-by-light scattering: Two-pion contributions, J. High Energy Phys. 04 (2017) 161.

[16] M. Hoferichter, B.-L. Hoid, B. Kubis, S. Leupold, and S. P. Schneider, Dispersion relation for hadronic light-by-light scattering: Pion pole, J. High Energy Phys. 10 (2018) 141.

[17] A. Gérardin, H. B. Meyer, and A. Nyffeler, Lattice calculation of the pion transition form factor with $N_f=2+1$ Wilson quarks, Phys. Rev. D **100**, 034520 (2019).

[18] J. Bijnens, N. Hermansson-Truedsson, and A. Rodríguez-Sánchez, Short-distance constraints for the HLbL contribution to the muon anomalous magnetic moment, Phys. Lett. B **798**, 134994 (2019).

[19] G. Colangelo, F. Hagelstein, M. Hoferichter, L. Laub, and P. Stoffer, Longitudinal short-distance constraints for the hadronic light-by-light contribution to $(g-2)_\mu$ with large-N_c Regge models, J. High Energy Phys. 03 (2020) 101.

[20] T. Blum, N. Christ, M. Hayakawa, T. Izubuchi, L. Jin, C. Jung, and C. Lehner, The hadronic light-by-light scattering contribution to the muon anomalous magnetic moment from lattice QCD, Phys. Rev. Lett. **124**, 132002 (2020).

[21] G. W. Bennett *et al.* (Muon g-2 Collaboration), Measurement of the negative muon anomalous magnetic moment to 0.7 ppm, Phys. Rev. Lett. **92**, 161802 (2004).

[22] B. Abi *et al.* (Muon g-2 Collaboration), Measurement of the positive muon anomalous magnetic moment to 0.46 ppm, Phys. Rev. Lett. **126**, 141801 (2021).

[23] D. P. Aguillard *et al.* (Muon g-2 Collaboration), Measurement of the positive muon anomalous magnetic moment to 0.20 ppm, Phys. Rev. Lett. **131**, 161802 (2023).

[24] S. Borsanyi *et al.*, Leading-order hadronic vacuum polarization contribution to the muon magnetic moment from lattice QCD, Nature (London) **593**, 51 (2021).

[25] F. V. Ignatov *et al.* (CMD-3 Collaboration), Measurement of the $e^+e^-\to\pi^+\pi^-$ cross section from threshold to 1.2 GeV with the CMD-3 detector, arXiv:2302.08834.

[26] R. H. Parker, C. Yu, W. Zhong, B. Estey, and H. Müller, Measurement of the fine-structure constant as a test of the standard model, Science **360**, 191 (2018).

[27] H. Davoudiasl and W. J. Marciano, Tale of two anomalies, Phys. Rev. D **98**, 075011 (2018).

[28] D. Hanneke, S. Fogwell, and G. Gabrielse, New measurement of the electron magnetic moment and the fine structure constant, Phys. Rev. Lett. **100**, 120801 (2008).

[29] D. Hanneke, S. F. Hoogerheide, and G. Gabrielse, Cavity control of a single-electron quantum cyclotron: Measuring the electron magnetic moment, Phys. Rev. A **83**, 052122 (2011).

[30] L. Morel, Z. Yao, P. Cladé, and S. Guellati-Khélifa, Determination of the fine-structure constant with an accuracy of 81 parts per trillion, Nature (London) **588**, 61 (2020).

[31] G. F. Giudice, P. Paradisi, and M. Passera, Testing new physics with the electron g-2, J. High Energy Phys. 11 (2012) 113.

[32] A. Crivellin, M. Hoferichter, and P. Schmidt-Wellenburg, Combined explanations of $(g-2)_{\mu,e}$ and implications for a large muon EDM, Phys. Rev. D **98**, 113002 (2018).

[33] J. Liu, C. E. M. Wagner, and X.-P. Wang, A light complex scalar for the electron and muon anomalous magnetic moments, J. High Energy Phys. 03 (2019) 008.

[34] B. Dutta and Y. Mimura, Electron $g-2$ with flavor violation in MSSM, Phys. Lett. B **790**, 563 (2019).

[35] X.-F. Han, T. Li, L. Wang, and Y. Zhang, Simple interpretations of lepton anomalies in the lepton-specific inert two-Higgs-doublet model, Phys. Rev. D **99**, 095034 (2019).

[36] M. Endo and W. Yin, Explaining electron and muon $g-2$ anomaly in SUSY without lepton-flavor mixings, J. High Energy Phys. 08 (2019) 122.

[37] M. Bauer, M. Neubert, S. Renner, M. Schnubel, and A. Thamm, Axion-like particles, lepton-flavor violation and a new explanation of a_μ and a_e, Phys. Rev. Lett. **124**, 211803 (2020).

[38] M. Badziak and K. Sakurai, Explanation of electron and muon $g-2$ anomalies in the MSSM, J. High Energy Phys. 10 (2019) 024.

[39] A. E. Cárcamo Hernández, S. F. King, H. Lee, and S. J. Rowley, Is it possible to explain the muon and electron $g-2$ in a Z' model?, Phys. Rev. D **101**, 115016 (2020).

[40] C. Cornella, P. Paradisi, and O. Sumensari, Hunting for ALPs with lepton flavor violation, J. High Energy Phys. 01 (2020) 158.

[41] W. Abdallah, R. Gandhi, and S. Roy, Understanding the MiniBooNE and the muon and electron $g-2$ anomalies with a light Z' and a second Higgs doublet, J. High Energy Phys. 12 (2020) 188.

[42] M. Ashry, K. Ezzat, and S. Khalil, Muon $g-2$ anomaly in a left-right model with an inverse seesaw mechanism, Phys. Rev. D **107**, 055044 (2023).

[43] M. I. Ali, M. Chakraborti, U. Chattopadhyay, and S. Mukherjee, Muon and electron $(g-2)$ anomalies with non-holomorphic interactions in MSSM, Eur. Phys. J. C **83**, 60 (2023).

[44] J. Cao, L. Meng, and Y. Yue, Electron and muon anomalous magnetic moment in the $\mathbb{Z}_3$-NMSSM, Phys. Rev. D **108**, 035043 (2023).

[45] J. Kawamura, S. Raby, and A. Trautner, Complete vector-like fourth family and new U(1)' for muon anomalies, Phys. Rev. D **100**, 055030 (2019).

[46] J. Kawamura, S. Raby, and A. Trautner, Complete vector-like fourth family with U(1)': A global analysis, Phys. Rev. D **101**, 035026 (2020).

[47] B. Allanach, F. S. Queiroz, A. Strumia, and S. Sun, Z' models for the LHCb and $g-2$ muon anomalies, Phys. Rev. D **93**, 055045 (2016); Phys. Rev. D **95**, 119902(E) (2017).

[48] W. Altmannshofer, M. Carena, and A. Crivellin, $L_\mu - L_\tau$ theory of Higgs flavor violation and $(g-2)_\mu$, Phys. Rev. D **94**, 095026 (2016).

[49] E. Megias, M. Quiros, and L. Salas, $g_\mu - 2$ from vector-like leptons in warped space, J. High Energy Phys. 05 (2017) 016.

[50] S. Raby and A. Trautner, Vectorlike chiral fourth family to explain muon anomalies, Phys. Rev. D **97**, 095006 (2018).

[51] L. Darmé, K. Kowalska, L. Roszkowski, and E. M. Sessolo, Flavor anomalies and dark matter in SUSY with an extra U(1), J. High Energy Phys. 10 (2018) 052.

[52] H. Kulkarni and S. Raby, An $SU(5) \times U(1)'$ SUSY GUT with a "vector-like chiral" fourth family to fit all low energy data, including the muon g-2, J. High Energy Phys. 05 (2023) 152.

[53] H. M. Lee, J. Song, and K. Yamashita, Seesaw lepton masses and muon $g-2$ from heavy vector-like leptons, J. Korean Phys. Soc. **79**, 1121 (2021).

[54] H. M. Lee and K. Yamashita, A model of vector-like leptons for the muon $g-2$ and the W boson mass, Eur. Phys. J. C **82**, 661 (2022).

[55] S. Q. Dinh and H. M. Tran, Muon g-2 and semileptonic B decays in the Bélanger-Delaunay-Westhoff model with gauge kinetic mixing, Phys. Rev. D **104**, 115009 (2021).

[56] Q. Zhou, X.-F. Han, and L. Wang, The CDF W-mass, muon $g-2$, and dark matter in a $U(1)_{L_\mu - L_\tau}$ model with vector-like leptons, Eur. Phys. J. C **82**, 1135 (2022).

[57] B. De, D. Das, M. Mitra, and N. Sahoo, Magnetic moments of leptons, charged lepton flavor violations and dark matter phenomenology of a minimal radiative Dirac neutrino mass model, J. High Energy Phys. 08 (2022) 202.

[58] D. Borah, M. Dutta, S. Mahapatra, and N. Sahu, Lepton anomalous magnetic moment with singlet-doublet fermion dark matter in a scotogenic $U(1)_{L_\mu - L_\tau}$ model, Phys. Rev. D **105**, 015029 (2022).

[59] J. Aebischer, W. Altmannshofer, D. Guadagnoli, M. Reboud, P. Stangl, and D. M. Straub, B-decay discrepancies after Moriond 2019, Eur. Phys. J. C **80**, 252 (2020).

[60] M. Algueró, B. Capdevila, A. Crivellin, S. Descotes-Genon, P. Masjuan, J. Matias, M. Novoa Brunet, and J. Virto, Emerging patterns of new physics with and without lepton flavour universal contributions, Eur. Phys. J. C **79**, 714 (2019); Eur. Phys. J. C **80**, 511(A) (2020).

[61] A. K. Alok, A. Dighe, S. Gangal, and D. Kumar, Continuing search for new physics in $b \to s\mu\mu$ decays: Two operators at a time, J. High Energy Phys. 06 (2019) 089.

[62] M. Ciuchini, A. M. Coutinho, M. Fedele, E. Franco, A. Paul, L. Silvestrini, and M. Valli, New physics in $b \to s\ell^+\ell^-$ confronts new data on lepton universality, Eur. Phys. J. C **79**, 719 (2019).

[63] A. Datta, J. Kumar, and D. London, The B anomalies and new physics in $b \to se^+e^-$, Phys. Lett. B **797**, 134858 (2019).

[64] K. Kowalska, D. Kumar, and E. M. Sessolo, Implications for new physics in $b \to s\mu\mu$ transitions after recent measurements by Belle and LHCb, Eur. Phys. J. C **79**, 840 (2019).

[65] A. Arbey, T. Hurth, F. Mahmoudi, D. Martinez Santos, and S. Neshatpour, Update on the b → s anomalies, Phys. Rev. D **100**, 015045 (2019).

[66] D. Kumar, K. Kowalska, and E. M. Sessolo, Global Bayesian analysis of new physics in $b \to s\mu\mu$ transitions after Moriond-2019, arXiv:1906.08596.

[67] G. Hiller, C. Hormigos-Feliu, D. F. Litim, and T. Steudtner, Anomalous magnetic moments from asymptotic safety, Phys. Rev. D **102**, 071901 (2020).

[68] A. de Giorgi, L. Merlo, and S. Pokorski, The low-scale seesaw solution to the M_W and $(g-2)_\mu$ anomalies, Fortschr. Phys. **71**, 2300020 (2023).

[69] LHCb Collaboration, Measurement of lepton universality parameters in $B^+ \to K^+\ell^+\ell^-$ and $B^0 \to K^{*0}\ell^+\ell^-$ decays, Phys. Rev. D **108**, 032002 (2023).

[70] J. Kawamura and S. Raby, W mass in a model with vectorlike leptons and U(1)', Phys. Rev. D **106**, 035009 (2022).

[71] T. Aaltonen *et al.* (CDF Collaboration), High-precision measurement of the W boson mass with the CDF II detector, Science **376**, 170 (2022).

[72] P. A. Zyla *et al.* (Particle Data Group), Review of particle physics, Prog. Theor. Exp. Phys. **2020**, 083C01 (2020).

[73] M. Pospelov, Secluded U(1) below the weak scale, Phys. Rev. D **80**, 095002 (2009).

[74] J. P. Lees *et al.* (*BABAR* Collaboration), Search for a dark photon in e^+e^- collisions at *BABAR*, Phys. Rev. Lett. **113**, 201801 (2014).

[75] J. R. Batley *et al.* (NA48/2 Collaboration), Search for the dark photon in π^0 decays, Phys. Lett. B **746**, 178 (2015).

[76] R. Aaij *et al.* (LHCb Collaboration), Search for dark photons produced in 13 TeV pp collisions, Phys. Rev. Lett. **120**, 061801 (2018).

[77] J. P. Lees *et al.* (*BABAR* Collaboration), Search for invisible decays of a dark photon produced in e^+e^- collisions at *BABAR*, Phys. Rev. Lett. **119**, 131804 (2017).

[78] Y. M. Andreev *et al.* (NA64 Collaboration), Constraints on new physics in electron $g-2$ from a search for invisible decays of a scalar, pseudoscalar, vector, and axial vector, Phys. Rev. Lett. **126**, 211802 (2021).

[79] G. Mohlabeng, Revisiting the dark photon explanation of the muon anomalous magnetic moment, Phys. Rev. D **99**, 115001 (2019).

[80] M. Duerr, T. Ferber, C. Hearty, F. Kahlhoefer, K. Schmidt-Hoberg, and P. Tunney, Invisible and displaced dark matter signatures at Belle II, J. High Energy Phys. 02 (2020) 039.

[81] M. Duerr, T. Ferber, C. Garcia-Cely, C. Hearty, and K. Schmidt-Hoberg, Long-lived dark Higgs and inelastic dark matter at Belle II, J. High Energy Phys. 04 (2021) 146.

[82] A. M. Abdullahi, M. Hostert, D. Massaro, and S. Pascoli, Semi-visible dark photons below the electroweak scale, Phys. Rev. D **108**, 015032 (2023).

[83] C. Cazzaniga *et al.* (NA64 Collaboration), Probing the explanation of the muon (g-2) anomaly and thermal light dark matter with the semi-visible dark photon channel, Eur. Phys. J. C **81**, 959 (2021).

[84] R. Dermisek and A. Raval, Explanation of the Muon g-2 anomaly with vectorlike leptons and its implications for Higgs decays, Phys. Rev. D **88**, 013017 (2013).

[85] F. Jegerlehner and A. Nyffeler, The Muon g-2, Phys. Rep. **477**, 1 (2009).

[86] J. Kawamura, S. Okawa, and Y. Omura, W boson mass and muon $g-2$ in a lepton portal dark matter model, Phys. Rev. D **106**, 015005 (2022).

[87] M. E. Peskin and T. Takeuchi, Estimation of oblique electroweak corrections, Phys. Rev. D **46**, 381 (1992).

[88] M. E. Peskin and T. Takeuchi, A new constraint on a strongly interacting Higgs sector, Phys. Rev. Lett. **65**, 964 (1990).

[89] L. Lavoura and J. P. Silva, The Oblique corrections from vector—like singlet and doublet quarks, Phys. Rev. D **47**, 2046 (1993).

[90] R. Dermisek, J. Kawamura, E. Lunghi, N. McGinnis, and S. Shin, Leptonic cascade decays of a heavy Higgs boson through vectorlike leptons at the LHC, J. High Energy Phys. 10 (2022) 138.

[91] I. Maksymyk, C. P. Burgess, and D. London, Beyond S, T and U, Phys. Rev. D **50**, 529 (1994).

[92] W. Grimus, L. Lavoura, O. M. Ogreid, and P. Osland, The Oblique parameters in multi-Higgs-doublet models, Nucl. Phys. **B801**, 81 (2008).

[93] K. S. Babu, C. F. Kolda, and J. March-Russell, Implications of generalized Z—Z-prime mixing, Phys. Rev. D **57**, 6788 (1998).

[94] K. Harigaya, E. Petrosky, and A. Pierce, Precision electroweak tensions and a dark photon, arXiv:2307.13045.

[95] D. Curtin, R. Essig, S. Gori, and J. Shelton, Illuminating dark photons with high-energy colliders, J. High Energy Phys. 02 (2015) 157.

[96] A. V. Artamonov *et al.* (BNL-E949 Collaboration), Study of the decay $K^+ \to \pi^+\nu\bar{\nu}$ in the momentum region $140 < P_\pi < 199$ MeV/c, Phys. Rev. D **79**, 092004 (2009).

[97] E. Cortina Gil *et al.* (NA62 Collaboration), Search for production of an invisible dark photon in π^0 decays, J. High Energy Phys. 05 (**2019**) 182.

[98] E. Cortina Gil *et al.* (NA62 Collaboration), Search for a feebly interacting particle X in the decay $K^+ \to \pi^+X$, J. High Energy Phys. 03 (**2021**) 058.

[99] E. Cortina Gil *et al.* (NA62 Collaboration), Search for π^0 decays to invisible particles, J. High Energy Phys. 02 (2021) 201.

[100] S. Carrazza, C. Degrande, S. Iranipour, J. Rojo, and M. Ubiali, Can new physics hide inside the proton?, Phys. Rev. Lett. **123**, 132001 (2019).

[101] G. D. Kribs, D. McKeen, and N. Raj, Breaking up the proton: An affair with dark forces, Phys. Rev. Lett. **126**, 011801 (2021).

[102] A. W. Thomas, X. G. Wang, and A. G. Williams, Constraints on the dark photon from deep inelastic scattering, Phys. Rev. D **105**, L031901 (2022).

[103] M. McCullough, J. Moore, and M. Ubiali, The dark side of the proton, J. High Energy Phys. 08 (2022) 019.

[104] A. W. Thomas, X. Wang, and A. G. Williams, Sensitivity of parity-violating electron scattering to a dark photon, Phys. Rev. Lett. **129**, 011807 (2022).
[105] P. D. Bolton, F. F. Deppisch, and P. S. Bhupal Dev, Neutrinoless double beta decay versus other probes of heavy sterile neutrinos, J. High Energy Phys. 03 (2020) 170.
[106] B. Batell, N. Lange, D. McKeen, M. Pospelov, and A. Ritz, Muon anomalous magnetic moment through the leptonic Higgs portal, Phys. Rev. D **95**, 075003 (2017).
[107] A. Anastasi *et al.*, Limit on the production of a low-mass vector boson in $e^+e^- \to U\gamma$, $U \to e^+e^-$ with the KLOE experiment, Phys. Lett. B **750**, 633 (2015).
[108] B. Batell, A. Freitas, A. Ismail, and D. Mckeen, Flavor-specific scalar mediators, Phys. Rev. D **98**, 055026 (2018).
[109] T. Abe *et al.* (Belle-II Collaboration), Belle II technical design report, arXiv:1011.0352.
[110] W. Altmannshofer *et al.* (Belle-II Collaboration), The Belle II physics book, Prog. Theor. Exp. Phys. **2019**, 123C01 (2019); Prog. Theor. Exp. Phys. **2020**, 029201(E) (2020).
[111] Y.-S. Liu, D. McKeen, and G. A. Miller, Electrophobic scalar boson and muonic puzzles, Phys. Rev. Lett. **117**, 101801 (2016).
[112] E. M. Riordan *et al.*, A search for short lived axions in an electron beam dump experiment, Phys. Rev. Lett. **59**, 755 (1987).
[113] J. D. Bjorken, S. Ecklund, W. R. Nelson, A. Abashian, C. Church, B. Lu, L. W. Mo, T. A. Nunamaker, and P. Rassmann, Search for neutral metastable penetrating particles produced in the SLAC beam dump, Phys. Rev. D **38**, 3375 (1988).
[114] M. Davier and H. Nguyen Ngoc, An unambiguous search for a light Higgs boson, Phys. Lett. B **229**, 150 (1989).
[115] A. Tumasyan *et al.* (CMS Collaboration), Inclusive nonresonant multilepton probes of new phenomena at $\sqrt{s} = 13$ TeV, Phys. Rev. D **105**, 112007 (2022).
[116] A. M. Sirunyan *et al.* (CMS Collaboration), Search for physics beyond the standard model in multilepton final states in proton-proton collisions at $\sqrt{s} = 13$ TeV, J. High Energy Phys. 03 (2020) 051.
[117] J. Liu, N. McGinnis, C. E. M. Wagner, and X.-P. Wang, A light scalar explanation of $(g-2)_\mu$ and the KOTO anomaly, J. High Energy Phys. 04 (2020) 197.